Article

Palaeoenvironmental Conditions of the Upper Middle Pleistocene Warm Intervals in the Upper Volga Region, Northwestern Russia, Based on Palynological, Paleocarpological and Quantitative Geochronological Data

Andrei Panin [1], Evgeny Konstantinov [1], Olga Borisova [1], Inna Zyuganova [1], Dmitrii Baranov [1], Natalia Karpukhina [1], Anna Utkina [1,*], Natalia Naryshkina [1] and Redzhep Kurbanov [1,2]

[1] Institute of Geography Russian Academy of Sciences, Staromonetny Lane 29, 119017 Moscow, Russia; a.v.panin@igras.ru (A.P.); eakonst@igras.ru (E.K.); olgakborisova@gmail.com (O.B.); dm_baranov@igras.ru (D.B.); nvkarpukhina@igras.ru (N.K.); naryshkina@igras.ru (N.N.); inna0110@gmail.com (I.Z.); roger.kurbanov@gmail.com (R.K.)
[2] Faculty of Geography, Lomonosov Moscow State University, Leninskiye Gory 1, 119899 Moscow, Russia
* Correspondence: utkina@igras.ru

Abstract: The climatostratigraphic scale of the Upper Middle Pleistocene in the northwest of the East European Plain contains a number of controversial issues, one of which is the position of the Likhvin (Holstein) Interglacial and lesser warm (interstadial) climatic events. To approach this problem, we have studied two sections of Quaternary deposits, Bolshaya Kosha (a well-known and long-studied natural exposure) and Nazarovo (a new, previously unknown section studied in a borehole), in which warm intervals of the Middle Pleistocene are recognized. In both sections, we performed lithological and paleobiological (carpological, spore-pollen) analyses and luminescence dating. In the Bolshaya Kosha section, seeds of the extinct species *Caulinia goretskyi* were revealed, which allowed us to attribute the obtained IRSL (ca 250–260 ka) dates to the post-Likhvin Bolshaya Kosha interstadial. The sum of data let us propose that both our IRSL and recently published ^{230}Th/U dates (ca 240–290 ka) underestimate the age by 10–15%, and the post-Likhvin Kosha interstadial deposits were formed in the late MIS 9. In the Nazarovo section, palynological study showed the conditions of a relatively warm interstadial, with a change in the composition of vegetation from northern to middle taiga forests. According to IRSL dating, the section was formed in the MIS 10 late glacial between 330–370 ka. The two studied interstadials bracket the Likhvin (Holstein) Interglacial and sedimentary units in the Bolshaya Kosha section are proposed to have formed in MIS 9e.

Keywords: thorium–uranium dating; IRSL; spore/pollen analysis; paleocarpology; Likhvin interglacial; Holstein interglacial; Kosha interstadial

1. Introduction

At present, one of the most significant problems of stratigraphy is the correlation of continental and marine sedimentation archives, as well as the linking of regional stratigraphic subdivisions to the global isotope–oxygen scale. Within the framework of this general task, there are a number of specific problems for the Middle Pleistocene of the East European Plain, among which one of the most important is the determination of the rank of warming episodes in the second half of the Middle Pleistocene and the chronological position of the Likhvin Interglacial (Holstein in Central Europe, see Table 1). Deposits of the Likhvin epoch are confidently identified by palaeobotanical methods (spore-pollen, carpological), but the position of this epoch on the time scale of MIS 9 or MIS 11 is still unclear (Table 1; see also the review in [1]). The data on warm climatic intervals between the Likhvin and the last glaciation of the Middle Pleistocene, the Moscow glaciation (Saale in Europe, MIS 6), could add clarity to this problem.

Table 1. Latest stratigraphic schemes of the Middle Neopleistocene in the central European part of Russia and their matching to marine isotope stages (MIS) and stratigraphic subdivisions of Eastern and Central Europe.

MIS [1]	ISC [2]	GSCR [3]	Eastern Europe			Central Europe		
			European Russia [4]	European Russia [5]	Belarus [6]	Poland [7]	Germany [8]	
6	Middle Pleistocene	Middle Neo-pleistocene	Dnieper	Moscow	Dnieperian II (Prypec)	Odranian		Drenthe + Warthe
7			Kamenka	Gorki	Shklovian	Lublinian	Saalian complex	Schoningen
8			Pechora	Vologda	Cooling	Krznanian		? (Cooling)
9			Likhvin	Chekalin	Smolenskian	Zbójnian		Reinsdorf
10				Kaluga	Cooling	Liwiecian		Fuhne
11			Oka	Likhvin	Alexandrian	Mazovian	Holsteinian	
12		Lower Neo-pleistocene		Oka	Berezinian	Sanian-2	Elsterian	

[1] MIS = marine isotope stages [2]; [2] ISC = international stratigraphic scale [3]; [3] GSCR = general stratigraphic scale of Russia [4]; [4] [5]; [5] [1,6]; [6] [7]; [7] [8]; [8] [9].

The solution to the problem of the Upper Middle Pleistocene stratigraphic scale is hampered by the lack of a reliable geochronological basis for paleobotanically studied sections. We attempted to apply the luminescence dating technique to two sedimentary sections in the Upper Volga basin, containing deposits of the Middle Pleistocene warming periods. The first is the eroded valley side of the lower reaches of the Bolshaya Kosha River (the left tributary of the Volga), containing buried organogenic sediments that have attracted researchers since the late 19th to the early 20th centuries [10,11] and have been repeatedly studied since the 1940s (see description of the history of the study in Section 2.2). This natural outcrop is known in the literature as the Bolshaya Kosha section (Figure 1). Another name sometimes found in the literature is the section "at the Pogost (small settlements with a church and a graveyard) of Elijah the Prophet" (simplified Russian—"Ilya Prorok"). Particular attention was drawn to the thick unit of lake/marsh sediments, in which a number of researchers identified layers of the Likhvin epoch, as well as transitional layers to the subsequent glacial part of the 100 ka climatic rhythm. Recently, ^{230}Th/U dates related to MIS 8 were published for organogenic deposits of this section [12]. We tried to clarify the geochronology of the section by IRSL dating and also carried out a paleocarpological analysis of the upper part of the organogenic sequence, which had not previously been studied by this method, in order to clarify its position relative to the Likhvin Interglacial.
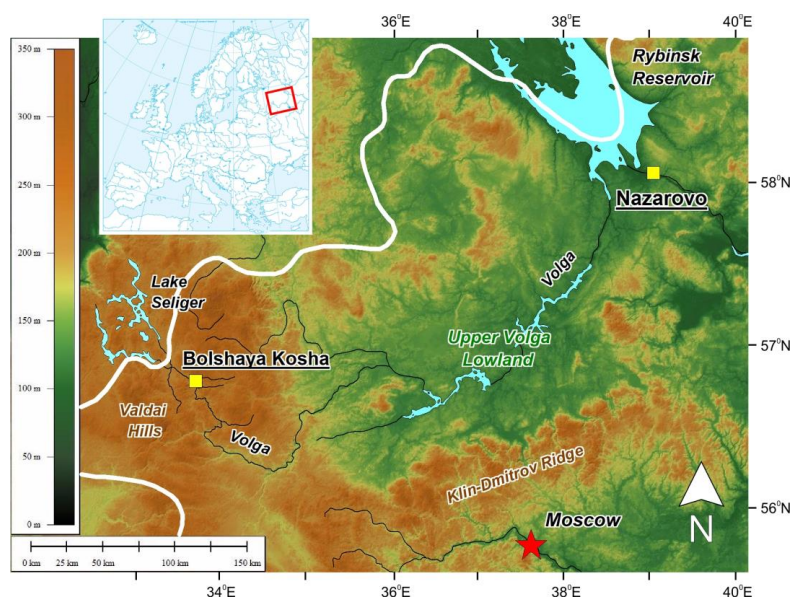
Figure 1. Location map. White line is the LGM boundary, after [13]. The MIS 6 ice sheet boundary is to the south and east, outside the figure.

The second section is Nazarovo in the upper Volga valley, near the town of Rybinsk (Figure 1). This section has not been studied previously, since weakly humified fine-grained sediments suitable for pollen analysis are not exposed on the surface. They were discovered during drilling in the bottom of a gravel quarry (core 19547), at the previously studied section in the quarry wall (pit 063). The spore-pollen analysis performed on these deposits provides new data on interstadial warmings of the late Middle Pleistocene, information about which is still extremely rare, especially with geochronological support. For this section, a representative series of IRSL dates was obtained, which makes it possible to verify geochronological data for the Bolshaya Kosha (Ilya Prorok) section, where there are reliably substantiated Likhvin deposits.

The purpose of this paper is to clarify the position of the warm climatic intervals of the second half of the Middle Pleistocene in the East European Plain, on the basis of geochronometric data and paleobotanical study of the two above sections.

2. Materials and Methods

2.1. Location of the Sections

The Bolshaya Kosha (Ilya Prorok) section is located within the southeastern slope of the Valdai Upland, at the confluence of the Bolshaya Kosha and Volga rivers (Figures 1 and 2A). The interfluves are dominated by gently undulating and rolling terrain of glacial and glacio-fluvial sedimentation, complicated by kames and eskers. Our clearing, IP-2015 (height of the edge—218 m asl, coordinates—N 56.75504°, E 33.70382°), was laid on the right bank of the Bolshaya Kosha River, at the top of the river bend, within a steep (15–30°) erosion slope 16 m high above the low water level in the river. According to the map of Quaternary deposits by T.I. Stolyarova [14], the outcrop exposes the structure of the area of glacio-fluvial accumulation (outwash plain) from the end of the Middle Pleistocene, located at altitudes of 212–220 m ASL. The average elevations of the interfluve surfaces adjacent to the Bolshaya Kosha valley are 230–235 m ASL, the bottom of the valley is 198–200 m ASL.

The valley side at the clearing site was covered with forest. The thickness of the slope cover was 0.5–1.0 m. Throughout the entire length of the section, the slope cover was completely removed. The width of the clearing varied from 1 to 2 m. Samples were taken, layer by layer, for lithological and geochemical studies, paleocarpological analysis, and OSL dating.
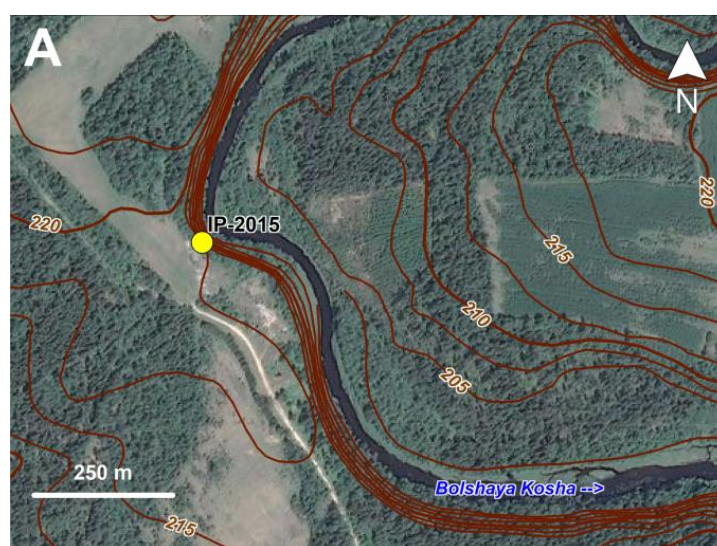
Figure 2. *Cont.*

Figure 2. Position of sections IP-2015 at Bolshaya Kosha (**A**) and 19547 at Nazarovo (**B**) in local topography. Contour lines drawn at intervals of 2.5 m (**A**) and 5 m (**B**).

The Nazarovsky quarry is located on the left bank of the Volga River, downstream of Rybinsk (Figures 1 and 2B). The quarry is located on an uneven surface with elevations of 94–100 m ASL, covered by MIS 6 moraine and glacio-fluvial deposits of the same age [15]. The section is located at 94 m ABS, 7–8 m above the natural level of the Volga (now the level is raised by about 1.5 m, due to the backwater from the Gorky Reservoir). Initially, the 4.5 m wall of the sand and gravel quarry, pit 063, was investigated. Then a 5.5 m deep borehole was drilled at the base of the clearing, so that the total depth of the section reached 10 m. It was in the borehole that a 135 cm thick layer of slightly humified loam was found and subjected to spore-pollen analysis.

2.2. Study History of the Bolshaya Kosha (Ilya Prorok) Section

The Bolshaya Kosha outcrop (Ilya Prorok) has a long history of investigation. The main methods used to study the stratigraphy of this section in the 20th century were palaeobotanical. K.K. Markov [16] interpreted the lake-marsh sediments as interglacial Mikulinian sediments (Eemian, MIS 5e), based on the results of spore-pollen analysis. A.I. Moskvitin first considered these sediments as Riss-Würmian [17], then as Odintso-vian (equivalent to MIS 7 in the stratigraphic scale of that time) [18], and later attributed them to the initial stage of the Kalinin glaciations (MIS 4), citing this section as a clas-sical location of sediments of the Upper Volga Interstadial (equivalent to MIS 5c) [19]. T.I. Stolyarova [20], based on the principle of superposition and the location of the Valdai glacia-tion boundary, correlated the inter-till layers with the Odintsovo interglaciation (MIS 7). These inter-till layers were found in a single section in 1991 and were not observed upstream and downstream of the river (Figure 3A). In [21], the outcrop at Bolshaya Kosha was studied in more detail and organogenic deposits were reliably found to be wedging out upstream and downstream along the outcrop (Figure 3B). M.A. Nedoshivina conducted a palynological study of section in 1991, which showed the presence of up to 15% pollen in warm-temperate broad-leaved species (*Tilia*, *Quercus*, *Carpinus*, *Ulmus*, and *Corylus*) and of *Picea* (up to 25%) [21]. According to this researcher, such composition of vegetation indicates the interglacial character of lacustrine deposits and is characteristic of the Likhvin Interglacial (Holsteinian in Central Europe) [21].
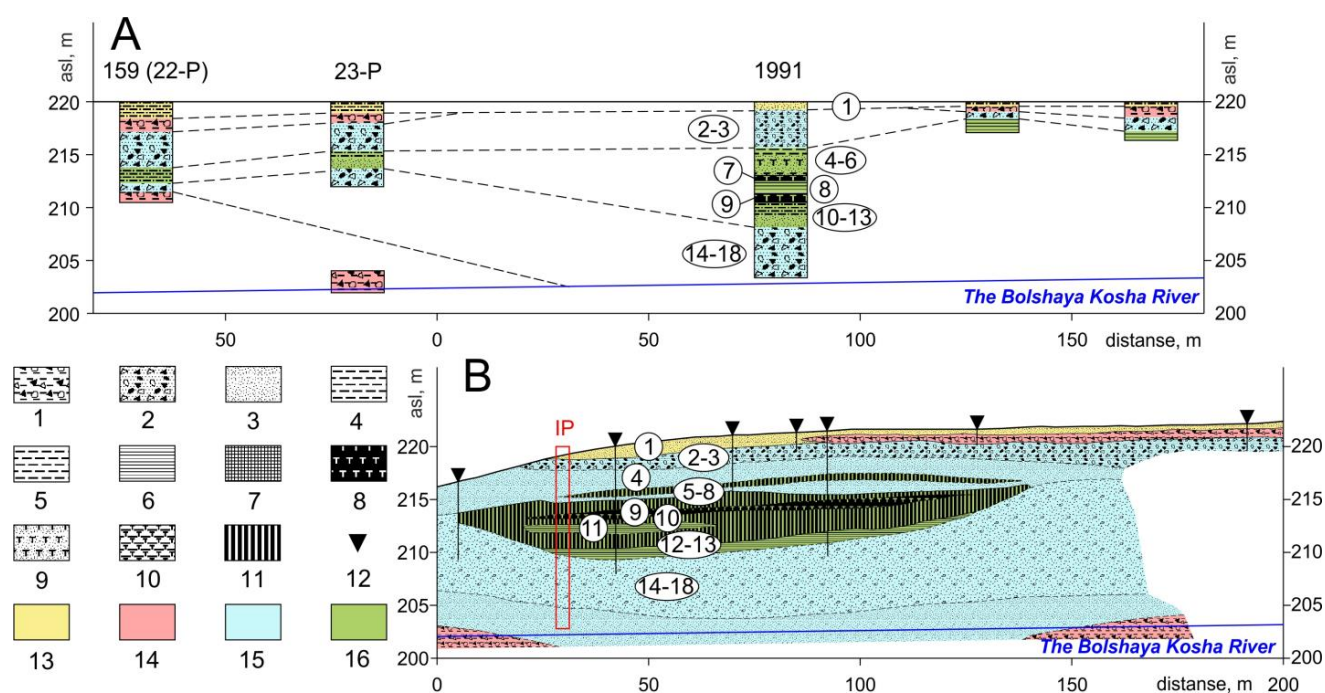
Figure 3. Bolshaya Kosha (Ilya Prorok) exposure, as documented in [20] (**A**) and [21] (**B**). Red rectangle shows the section IP-2015 studied in this paper. Circled numbers are units recognized in IP-2015 section. Legend: Lithology: 1—diamicton, 2—sand with gravel and pebbles, 3—sand, 4—silt, 5—loam (silty clay), 6—clay, 7—argillite, 8—peat, 9—peaty sand, 10—peaty loam, 11—gittya; 12—pits and cores. Genesis: 13—aeolian, 14—glacial, 15—fluvial and/or fluvioglacial, 16—lacustrine and swamp deposits.

The palynological record of the section on the Bolshaya Kosha River was produced by V.P. Grichuk in 1960 [22,23]. Local pollen assemblage zones (LPAZs) corresponding to the Likhvin Interglacial, the post-Likhvin cooling, and the subsequent relative warming were identified. In the LPAZ associated with the layer of compact gyttja (8.5–9.6 m depth), the maximum pollen content of fir (*Abies*) and hornbeam (*Carpinus*), and high pollen content of other broad-leaved trees (oak, linden, and elm), were observed. Grichuk [23] referred this zone to the optimum of the Likhvin Interglacial. Above the interglacial sequence, palynospectra indicated periglacial vegetation and significant cooling. The increased content of spruce and fir pollen and the appearance of single pollen grains of *Quercus* and *Tilia* allowed Grichuk [23] to identify relative warming in the studied section, which he called the Kosha interstadial (see also Table 2). Palynospectra of the overlying peat layer apparently reflected further climate cooling [23].

In the early 2000s, palynological studies of the section were carried out by L.V. Savelyeva and V.V. Razina. The results were published in [12]. For the buried lacustrine deposits in the lower part of the section (depth 8.2–10.6 m, materials of 2001), the LPAZ sequence was obtained, similar to the PAZ sequence of the Likhvin Interglacial, identified earlier in the same location by V.P. Grichuk [23]. The pollen data characterised the interglacial, including its climatic optimum (8.5–9.0 m depth) [12]. In the corresponding LPAZ (L-3), relatively high pollen contents of hornbeam (up to 15% of the terrestrial pollen sum) and fir (up to 12%) were noted. The simultaneous culmination of hornbeam and fir pollen contents against the background of the predominance of spruce and pine pollen, and warm temperate broad-leaved trees (*Quercus, Ulmus, Tilia, Corylus*), is a characteristic feature for the optimal phase of the Likhvin Interglacial on the East European Plain [23]. Nevertheless, the *Abies* pollen content in the layer corresponding to the Likhvin climatic optimum on the pollen diagram of the Bolshaya Kosha, according to Grichuk [23], reaches almost 30% of the pollen sum, culminating together with *Carpinus* pollen. This difference possibly indicates

that the pollen sequence from the 2001 section by Savelyeva and Razina lacks the warmest part of the Likhvin Interglacial optimum, due to a break in the sediment sequence, where the distinct boundary is fixed at a depth of 8.70 m.

Palynological characteristics of the overlying buried lacustrine deposits (6.30–7.85 m depth) were obtained from samples from the section studied in 2003. Palynological data characterise a relatively slight warming of interstadial rank, with dominance of pine forests, separated from the interglacial by cooling with sharp predominance of birch forests with small participation of spruce, the presence of cryophilic shrubs (*Betula nana*, *Alnus fruticosa*) and the expansion of open herbaceous communities of *Artemisia*, Chenopodiaceae and Poaceae. This cooling was attributed to the transition phase between the Likhvin interglaciation and the Dnieper glaciation [12]. In the pollen diagram of the Bolshaya Kosha section studied by V.P. Grichuk [23], the first warming, separated by the cooling phase from the Likhvin interglaciation, is represented somewhat more completely. In its late part, there was a significant admixture of spruce in the predominant pine and birch forests, where fir, larch, and alder (*Alnus incana* and *A. glutinosa*) occurred. This warming was named the Kosha interstadial in the Russian literature, based on this section [23].

In addition to pollen, plant macrofossils have been repeatedly studied in sections on the Bolshaya Kosha River. The earliest publications [16,19] on the peat horizon above the gyttja indicate the findings of macrofossils of the following plant taxa: *Carex* sp., *Menyanthes trifoliata*, *Potamogeton* spp. (two species), *Pinus sylvestris*, and *Betula nana*. The paper by I.I. Krasnov and T.D. Kolesnikova [24] provides a generalised list of macrofossils of predominantly eurythermal wetland plants. Such aquatic plant species as *Najas flexilis* and the far- eastern species *Potamogeton oxyphyllus*, which in subsequent studies were identified as the extinct species *Caulinia goretsqyi* and *P. sarjanensis*, respectively [12,25], were indicated in this study. Seeds of spruce *Picea abies* and megaspores of *Selaginella selaginoides* were identified. The authors [24] attributed this flora to the Mologa-Sheksna epoch (analogue of MIS 3).

Another re-examination of this section was carried out in the 1970s. Paleocarpologist F. Yu. Velichkevich [25] identified a local carpological assemblage (LCA) containing 24 taxa of predominantly wetland plants from a layer of dense gyttja at a depth of 9.7–11 m. For the first time, extinct species (*P. sarjanensis*, *Caulinia goretsqyi*, *C. interglacialis*) were identified in the studied section. In addition, macrofossils of *Abies* cf. *alba* and megaspores of *Salvinia natans* were found. Referring to the findings of macrofossils of *Acer* sp. and *Aldrovanda* sp. [21], Velichkevich [25] attributed this LCA to the Likhvin Interglacial. According to [25], considered LCA was poorer than the Likhvin carpological assemblages from other sections, including the stratotypic section near Chekalin on the Oka River. This can be explained by the fact that in the Bolshaya Kosha section, the sediments of the warmest part of the interglacial are represented by argillite (dense gyttja), while findings of the most representative carpological assemblages are usually confined to peaty lake-mire sediments [25].

Later, in the early 2000s, Velichkevich analysed samples from the peat and gyttja layer at a depth of 6.7–7.4 m. This interval was attributed, on the basis of pollen data, to the transitional stage from interglaciation to glaciation [12]. Velichkevich identified almost 40 taxa of plant macrofossils. Tree species are represented by spruce, pine, larch, and birch. Several extinct Pleistocene species (*Potamogeton perforatus*, *P. sarjanensis*, *Caulinia goretskyi*), peculiar to the pre-Dnieper interglacial floras of the East European Plain, were represented among aquatic plants [25]. Velichkevich suggested that the considered LCA could be attributed to the post-optimal and final phases of the Likhvin Interglacial [12].

The lack of geochronometric data left unresolved questions about the absolute age of the lacustrine-marsh strata and, accordingly, their belonging to certain stratigraphic horizons. Despite the active development of the radiocarbon method since the 1950s, this section has received little attention. This was probably due to the fact that most researchers compared the lacustrine deposits to the middle or early Late Pleistocene, which is much older than the radiocarbon dating limit. However, in 1961–1962, Z.V. Yatskevich, on the

basis of radiocarbon dating of wood (date of about 32 ka BP), suggested that the peaty sediments belong to the Mologa-Sheksna epoch (MIS 3) [24]. In relation to this, the results of uranium–thorium dating carried out by a group of researchers led by F.E. Maximov, are of particular value [12]. A ^{230}Th/U age no older than 287 ± 39/27 ka was obtained for the peaty loam in the lower part of the lacustrine-marsh strata, attributed to deposits of the first half of the Likhvin Interglacial. For the peat layer deposited during the transitional phases from the Likhvin Interglacial to the Dnieper glaciation (middle part of the strata), ^{230}Th/U isochron ages of 237 ± 19/12 ka and 243 ± 12/8 ka were obtained [12]. The dates confirm that these interglacial deposits should be attributed to the Middle, but not to the Late Pleistocene. At the same time, the question remains open as to which of the Middle Pleistocene warming periods the accumulation of these sediments belongs. A number of researchers believe that the climatostratigraphy of the second half of the Middle Pleistocene was more complex than is reflected in the existing schemes (see Table 2 as an example).

Table 2. Detailed succession of paleogeographic events in the Middle Neopleistocene (after [26]).

Event	Climate
Moscow Glaciation (late stage)	Cold
Kostroma interstadial	Relatively warm
Moscow Glaciation (early stage)	Cold
Short-term climate fluctuations	Cooling Warming Cooling
Gorki Interglacial	Warm
Dnieper Glaciation	Cold
Short-term climate fluctuations	Cooling Maryino warming Tegliatsi (Kaluga) cooling Bulatovo warming Cooling Kosha warming Cooling
Likhvin Interglacial [1]	Warm

[1] V.V.Pisareva stands for MIS 11 age of the Likhvin Interglacial (pers. comm.).

In spite of the long history of research and the large amount of accumulated knowledge, questions about the number and rank of the thermochrons to which organogenic sediments correspond in the section remain open. The reasons for such a discussion are the presence of hiatuses in the lacustrine deposits and in the section as a whole, facies heterogeneity, poor exposure, and the landslide character of the valley side, which makes it difficult to work on the outcrop and complicates the correlation of the portions of the outcrop cleaned by different authors in different years. It is worth noting that until recently [27], the literature did not provide a detailed description of the structure or the properties of sediments in the section, supported by analytical characteristics. In view of the above, attempts to assign the Ilya Prorok section the status of a parastratotype of the Likhvin Interglacial look premature [28,29]. Additional geochronological studies for the section are strongly required.

2.3. Paleobotanical and Lithological Methods

Pollen and spores were separated from the sediment following the Grichuk and Zaklinskaya [30] method, using a heavy liquid with a density of 2.25 g cm^{-3}, and were examined using a light microscope with a magnification of ×400. Calculation of pollen percentages was based on the total terrestrial pollen and spores sum—arboreal pollen (AP) plus non-arboreal pollen (NAP), plus spores. In each sample, 300–400 grains were counted

in order to ensure a statistically significant sample size, then samples were further scanned to detect rare palynomorphs. In addition, other biogenic microfossils (plant detritus, non-pollen palynomorphs, such as conifers stomata, Algae, etc.) from the same samples were registered, as well as redeposited Mesozoic and Quaternary spores, pollen and NPP.

Carpological analysis was carried out to determine the stratigraphic position of the studied sediments using the biostratigraphic method. This type of plant macrofossil analysis involves the identification of subfossil seeds, fruits, megaspores, and some other plant parts, such as needles and leaves [31]. In the Bolshaya Kosha 2015 section, 13 samples for carpological analysis were taken from the buried peat, peaty loams, and gyttja layers, at a depth of 10.4–4.2 m. Additionally, four samples of the buried peat were collected from the drill-hole near the studied exposure. The volume of each sample was 500–600 cm^3. Plant residue was extracted from the samples following V.P. Nikitin's work [31]. The plant macrofossils were examined using a stereomicroscope Altami SM II, in order to collect carpological remains, which were then identified by following atlases [32,33] and using the reference collection kept at the Laboratory of Stratigraphy and Paleontology of the "Research and Production Center for Geology", Belarus. A carpological diagram was made using TILIA and TILIA GRAPH software [34].

Loss on ignition at 550 °C (LOI 550) and quantitative elemental analysis were performed in the Laboratory of Mineral Matter Analysis at the Institute of Geology of Ore Deposits, Petrography, Mineralogy, and Geochemistry in the Russian Academy of Sciences (IGEM RAS), according to the standard technique [35]. The content of elements was determined on the Axios mAX advanced X-ray fluorescence spectrometer using powder samples compressed into tablets.

2.4. Luminescence Dating

Samples were collected in opaque plastic tubes that were covered with foil on both ends and taped to retain moisture. The sample preparation process is described in detail in [15]. It involved wet sieving to separate the sand fractions, then the chosen fraction was treated with 10% HCl and 10% H_2O_2, each for one hour, and then with 10% HF and 10% HCl, each for 20 min. A 2.58 g/cm^3 LST aqueous heavy liquid solution was used for quartz and feldspar separation. K-feldspar grains (the light fraction) were rinsed with distilled water, dried, and packed. Quartz grains (heavy fraction) were etched in 40% HF for one hour and then washed with 10% HCl for 20 min [36].

All measurements were performed using multi-grain aliquots at the Nordic Laboratory for Luminescence Dating in Risø, Denmark. Samples were measured in a Risø TL/OSL reader, model TLDA20, equipped with a calibrated beta source (dose rate 0.057–0.220 Gy/s) [37,38]. For quartz measurement, we used the single aliquot regenerative dose (SAR) procedure, which is described in [15]. We do not feature it here, since no definitive quartz age results are reported in this paper. Feldspar was measured using a post-IR IRSL SAR protocol [39,40]. Light detection was through a blue filter combination [41]. Then, 2-mm diameter aliquots mounted on stainless steel cups were first preheated (to 320 °C for 60 s following natural and regeneration doses, and to 310 °C for 60 s following test doses) and then stimulated by infrared light for 200 s at two temperatures; first 50 °C (IR$_{50}$ signal), then 290 °C (pIRIR$_{290}$ signal). No correction was made for possible pIRIR$_{290}$ [39–41] or IR$_{50}$ signal instability.

Radionuclide concentrations were measured using high-resolution gamma spectrometry [42,43]. Sample preparation involved drying at 100 °C for 24 h, ignition at 450 °C for 24 h, grinding, mixing with high viscosity wax, and casting in a cup-shaped mould. The spectrometers were calibrated using a combination of certified reference materials produced by Natural Resources Canada (NRCAN) and analytical grade K_2SO_4. The resulting ^{226}Ra, ^{232}Th, and ^{40}K activity concentrations were then converted to dry infinite-matrix dose rates, following Guerin et al. [44], assuming a 20 ± 10% loss of ^{222}Rn under field conditions. Water content corrections were based on [45] and cosmic ray contributions were derived from [46].

3. Results

3.1. Section Bolshaya Kosha (Ilya Prorok)

3.1.1. 3D Geometry of Organogenic Sediments in the Bolshaya Kosha (Ilya Prorok) Section

The Bolshaya Kosha River in the vicinity of the section undercuts a gently undulating southward-sloping plain, with elevations of 220–217 m ASL. Since previous studies had established that organogenic sediments along the left side of the Bolshaya Koshya valley lie in the form of a lens that wedges upstream and downstream (Figure 3), it was necessary to check whether this lens extends deep into the interfluve, in which case we could assume that it occupies a buried river valley. To test this, we drilled several boreholes along the profile along the edge of the valley (Figure 4).
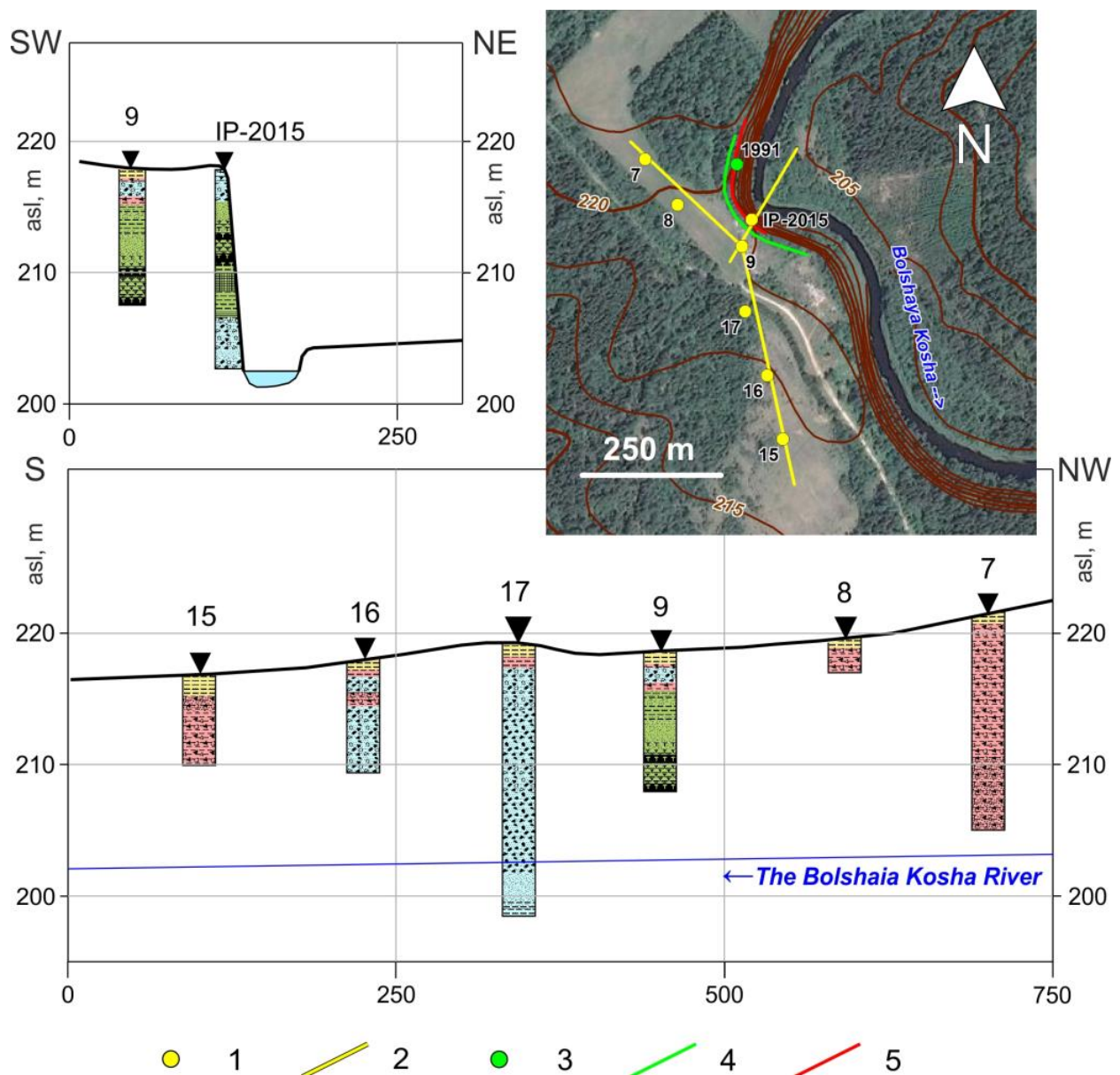
Figure 4. Geological structure of the interfluve in the area of Bolshaya Kosha (Ilya Prorok) exposure. Legend: 1—cores (this paper); 2—coring profile lines; 3—pit 1991 by [20] studied palynologically by [21]; 4—the outcrop studied by [20], see Figure 3A; 5—the outcrop studied by [21], see Figure 3B. See Figure 3 for lithological and genetic notations.

Organogenic sediments were encountered only in borehole 9, closest to the valley side outcrop IP-2015. This borehole generally follows the structure exposed at the valley side. Beneath the silts covering the surface, sands with large amounts of gravel and rubble (angular gravel), similar to those described in the section, were uncovered. At a depth of 2.5–3 m, a low thickness diamicton, described earlier in [21] (see also Figure 3B) but not encountered in the IP-2015 section [27], was found. Below, an interlayer of clayey loams, thin silty sands of grey and bluish-grey colour, with inclusions of wood and plant detritus in some places, generally similar sediments to that in section IP-2015 above the organogenic stratum, were exposed. The organogenic stratum itself, represented by dark brown peat, was revealed at a depth of about 8 m, which is a bit deeper than in section IP-2015.

Boreholes to the north of the section uncovered diamicton, which we consider to be the Moscow moraine (MIS 6), and in borehole 7, probably an older moraine. The moraine material was previously traced by [20,21], but its thickness was considered to be insignificant (the first metres) and it wedged out to the south. Indeed, boreholes 16 and 17, placed 200 and 100 m to the south of the section, revealed a complete absence of moraine deposits. Practically from the surface, there was a thick sand and gravel bed with a large amount of coarse clastic material, especially in the upper part. The thickness of these sediments was about 20 m, their bottom goes under the Bolshya Kosha River, and the underlying glacial sediments could not be reached. A similar situation with a thick sand and gravel bed was found by N.S. Chebotaryova et al. [21] (Figure 3B). To the south, in borehole 15 (500 m south of the section IP-2015), the moraine was uncovered again, and its thickness exceeded 5 m.

Thus, the organogenic stratum was proved to be lenticular. In the valley side outcrop, it was traced earlier for less than 150 m (Figure 3), and as one moves westwards from the present-day valley of the Bolshaya Kosha River, it is also wedged out. At the same time, a thick sand and gravel layer, with a total width along the river of 300–400 m, is traced for 150–200 m on both sides of the organogenic lens, and also goes under the interfluve (Figure 4). Apparently, the partial destruction of organogenic sediments was related to the formation of this sand and gravel bed. Above this stratum, the moraine material is either eroded or has a very limited distribution, whereas at a distance of more than 250–300 m from the organogenic lens, the moraine thickness increases significantly at the expense of the sand and gravel unit. This may indicate a relationship between the sand and gravel unit and the overlying till, with their formation during a single sedimentation event associated with the same deglaciation.

3.1.2. Structure of the IP-2015 Section and Facial Interpretation of the Lithostratigraphic Units

The section with a total height of 15.3 m contains 18 lithostratigraphic units (Table 3, Figure 5). At the base of the section (units 14–18), a coarse clastic stratified pack, dominated by gravel and pebble material with sandy matrix, single boulders, and lenses of cross-bedded sand, were encountered. LOI 550 is characterised by very low values (less than 1%), indicating the almost complete absence of organic matter in the sediment. Crystalline rocks of silicate and aluminosilicate composition (SiO_2 up to 76%, Al_2O_3 up to 11%) predominate the composition of the debris, but the fragments of carbonate rocks are also present. This is confirmed by the reaction of the material with HCl and increased values of CaO (up to 17%). The composition and textural features of this sediment pack correspond to turbulent flow conditions with high velocities and an unstable dynamic regime throughout the year. Such conditions of sedimentation in the study area are most likely to correspond to glacial meltwater flows that may correspond to the lowermost till found earlier at the river's low water level, upstream from the out section (Figure 3B).

Table 3. Lithostratigraphic units in section IP-2015.

Unit No. [1]	Description
1	Red loamy sand with gravel, pebbles, and small boulders (upper 30 cm without inclusions)
2	Coarse cross-bedded sand with gravel and pebbles
3	Pebble in sand and gravel matrix and inclusions of small boulders
4	Coarse laminated sand with inclusions of pebbles and gravel
5	Dark brown light peaty silt loam with inclusions of undecayed wood fragments
6	Grey fine sand with thin interlayers of peat
7	Dark brown (up to black) peat of high degree of decomposition, with thin interlayers of silt and fine sand and rare inclusions of wood fragments
8	Dark grey light peaty silt loam with rare inclusions of gravel, pebbles and small boulders, as well as with inclusions of poorly decomposed wood fragments (branches, small trunks)
9	Brownish-black peat of low decomposition, dense, leafy, with abundance of wood remains
10	Grey clay loam with argillite interlayers
11	Brownish-brown argillite with ferruginous films and crusts on the surfaces of laminae
12	Dark grey silty clay loam with blue tinge, with large spots of dark brown colour, with inclusion of grus (angular coarse sand and fine gravel) and fine sand, with interlayer of peaty black loam (2 cm)
13	Bluish-grey unlayered clay
14	Grey-brown clay loam with bluish and rusty spots, with inclusion of grus and angular gravel
15	Coarse-grained clayey brownish-reddish-pale oblique sand with inclusions of crushed stone
16	Pebble in sandy-gravel matrix and inclusion of boulders
17	Fine–medium cross-bedded sand
18	Pebble in sandy-gravel matrix and inclusion of small boulders

[1] Unit numbering is from top to bottom, numbers correspond to Figure 5.
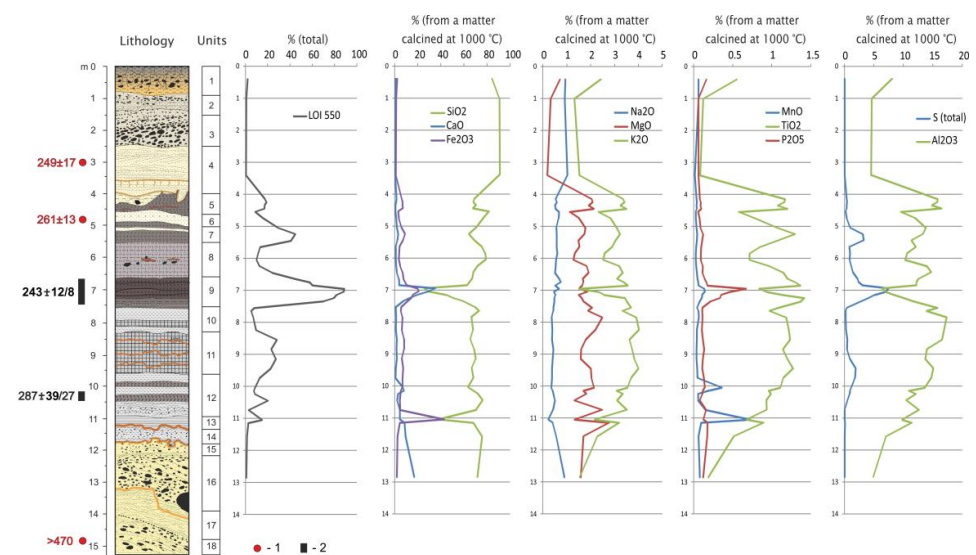
Figure 5. The structure of the IP-2015 section, dates, and chemical characteristics of the sediments. Units are lithostratigraphic units described in Table 3. LOI 550 = loss on ignition at 550 °C. Other plots show concentration of macroelements. Legend: 1—boulders, 2—pebble and gravel, 3—sand, 4—sand with cross lamination, 5—loamy sand, 6—loam, 7—argillite (ferruginous cemented peaty loam), 8—peat, 9—peaty loam, 10—clay, 11—wood remains, 12—ferruginous crusts, 13—roots, 14—position of IRSL (a, this paper) and ^{230}Th/U (b, after [12]), dates; ages are in ka.

Above the section lay a pack (units 10–13) of horizontally-bedded sediments with predominance of silty-clayey fractions in the grain size composition, without inclusion of large debris. This pack was characterised by high variability in organic matter content, with LOI 550 values varying from 3 to 28%. Higher LOI 550 values correspond to the layer of lithified platy reddish-brown mudstone (unit 11). Higher sulphur values (up to 9.5%) also correspond to this unit, which confirms the participation of a biogenic factor in sediment formation. The origin of argillite can be explained by diagenetic transformation of the initial organo-mineral lacustrine silt due to cementation by iron compounds, which is indicated by the presence of characteristic rusty films and crusts in the rock units. The underlying and overlying sediments in relation to layer 11 are unlithified clays and loams with an organic matter content of 3–8%, which can be considered as sediments of oligo-mesotrophic water bodies that periodically experienced short-term partial drying, as evidenced by lenses and thin peat interlayers in units 12 and 10. The upper part of the pack (the top of unit 10) is represented by an interbedding of loam, sandy loam, and peat, which indicates the lake shallowing at the final stage of its existence and its gradual transformation into a lowland bog. So, the composition and structure of the considered layer indicate the formation of sediments in the conditions of a relatively shallow water body with a very dynamic water level, which episodically reached complete shallowing and swamping.

The overlying layer 9 is represented by brownish-black leafy peat of low decomposition degree, with an abundance of wood remains, fragments of leaves, branches, and trunks. The proportion of organic matter in layer 9 is very high, with LOI 550 values in the range of 45–89%, with a maximum in the interlayer with an increased concentration of macrofossils of woody vegetation. The unit corresponds to the highest values of biogenic elements (sulphur and phosphorus) and the lowest values of silicon. Sand and silt interlayers and lenses are observed throughout the unit, indicating intermittent flow. The sediments described may correspond to the conditions of a small oxbow bog, located on a high floodplain and surrounded by woody and shrubby vegetation. During periods of high floods, once every few years, the bog received fine clastic material that formed characteristic interlayers within the peat deposit.

Unit 8 is represented by a peaty laminated loam with thin interlayers and lenses of sand and an organic matter content of 13 to 24%. Within unit 8, the interlayer at a depth of 5.8–6.3 m, characterised by the inclusion of pebbles, boulders, and fragments of tree trunks up to 10 cm in diameter, deserves special attention. The presence of boulders and pebbles in the loamy stratum can be explained, for example, by their transport on the roots of trees that fell into the river from the eroding banks, which were then carried by the flow and brought into the oxbow lake during high floods. Another mechanism is ice rafting.

The organo-mineral sediment pack (units 5–7) is an interbedding of highly decomposed peat, peaty loam, sand, and silts. The structure and composition of the deposits indicate the dominance of the bog regime at this stage, with dynamic alternation within lacustrine and alluvial regimes. The latter was characterised by a directional increase in the frequency and intensity of floods, which follows from an increase in the proportion of sandy sediment up in the section. The uneven top of the peaty loam of unit 5 attracts attention. This is a wedge-shaped deformation, in which sandy material from the overlying layer is embedded, which may indicate the impact of cryogenic processes following peat accumulation.

Unit 4 is represented by horizontally laminated (in some places cross-bedded) medium-coarse sand, with rare inclusion of gravel, pebbles, and a single inclusion of small boulder at the bottom of the layer. The bedding structure shows rhythmic alternation of 1–5 cm thick interlayers of dark silty sand and light well-washed medium-coarse sand. These facies characteristics allow unit 4 to be classified as an overbank alluvium, accumulated on a high floodplain in the vicinity of the river. Starting from layer 4, upwards in the section there is a sharp drop in the content of some lithogenic elements (Al_2O_3, TiO_2, K_2O, MgO, Fe_2O_3) and biogenic elements (S and P_2O_5). At the same time, the content of SiO_2 reaches its maximum, 91%.

Above unit 4, with a sharp erosion contact, is a coarse clastic stratified pack (units 2 and 3) with predominance of gravel-pebble size of debris, sandy matrix, and inclusion of small boulders. By their petrographic composition, the clasts are mainly crystalline rocks with a very low proportion of carbonates, confirmed by low CaO values (less than 2%). The coarse and purely sorted debris indicate the conditions of turbulent flow with unstable regime, which may indicate the glacio-fluvial origin of the sediments.

Unit 1, crowning the section, is represented by sandy loam with inclusions of pebbles and small boulders, which allows us to consider this layer as glacio-fluvial or glacio-lacustrine sediments. The upper 15 cm of the layer consist of homogeneous silt without inclusions, which may indicate its aeolian origin.

3.1.3. Luminescence Dating

Results of luminescence dating are presented in Table 4. Three OSL samples were collected at 3 m, 4.8 m, and 14.0 m. Dose rates for these samples are 1.2–1.6 Gy/ka for quartz and 2.1–2.5 Gy/ka for feldspar. Quartz OSL doses for all samples turned out to be around 220 Gy, so we consider quartz to be saturated. Estimated minimal quartz ages are ~140 ka for the first two samples (208446 and 208447) and ~180 ka for the last one (208448). Feldspar pIRIR doses for samples 208446 and 208447 exceed 600 Gy (629 and 647 Gy, respectively), and the dose of 208448 is greater than 1000 Gy, meaning that we could only estimate minimal pIRIR age for this sample. Feldspar IR doses for all these samples are around 400 Gy. Considering that IR signal was not fading corrected, the IR to pIRIR dose ratio does not indicate any differential bleaching of these two signals. The resulting pIRIR ages are 251 and 254 ka, respectively, corresponding to MIS 8. The minimal age for sample 208448 is 460 ka, which means that it was formed at least in MIS 12, if it was sufficiently bleached at deposition.

Table 4. Luminescence dating results. Minimal ages are reported with the '>' symbol.

Sample Code Lab	Depth, cm	Dose (Gy) and Total Aliquots						Quartz Dose Rate, Gy/ka *		Age, ka		
		Q		IR_{50}		$pIRIR_{290}$			Q	IR_{50}	$pIRIR_{290}$
208446	300	>220	6	390 ± 11	8	629 ± 32	8	1.56 ± 0.07	>141	156 ± 7	251 ± 17
208447	480	>220	6	388 ± 17	8	647 ± 19	8	1.60 ± 0.07	>137	153 ± 9	254 ± 13
208448	1400	>220	6	>400	6	>1000	6	1.20 ± 0.06	>183	>186	>466

* Dose rates for feldspar can be derived by adding 0.94 to quartz dose rates.

Luminescence dating results for the Nazarovo site (sections 063, 19547) were discussed in [15], together with the sediment structure. Both these sections represent a continuous sequence of sandy and silty sediment, with a coarse layer of an impenetrable mixture of boulders and gravel in its middle part. The upper part of this sequence is overlain by till that we consider having formed in MIS 6. The 10 OSL samples that were collected stratigraphically below this till show a densely grouped set of ages with a few outliers. Most of the ages fall into the range of 330–370 ka (MIS 10); two outliers, one in the bottom part (8 m from the start of the sequence) and another in the upper part (3 m from the start of the sequence), show dates of 250 ka and 270 ka, respectively (MIS 8). One more outlier at 1.5 m has an age of 480 ka. Pollen results from the lower part of the sequence (samples taken at 6 m) indicate a short-lived interstadial [47].

Assessment of the insufficient bleaching probability was performed to account for a possible age overestimation. Since pIRIR signals bleach more slowly than the IR_{50} signal [40], Murray et al. [48] proposed the use of these differential bleaching characteristics to investigate the degree of bleaching of quartz signals. Given that the two feldspar signals bleach at different rates, such investigation can be performed for them as well, by comparing the $pIRIR_{290}$ ages with the IR_{50} ages [49,50]. Such comparison for the Nazarovo site samples showed that there is no proof of differential bleaching of these two feldspar

signals, therefore we assume all these samples to be sufficiently bleached and to reflect their true age.

To see how the Ilya Prorok dataset compares with the previous one from Nazarovo, we added the Ilya Prorok feldspar ages to the previous IR/pIRIR Volga dataset from [15] (Figure 6). The only sample that lies significantly below the curve, and therefore shows some indication of its IR and pIRIR's differential bleaching, is 208448. It is worth noting that we do not know the doses and, consequently, the ages of both IR and pIRIR with high certainty (shown as minimal in Table 4). So, even though the difference between IR and pIRIR indicates a possible age overestimation for this sample, we cannot determine to what extent it could have been overestimated. The other two show good agreement with the rest of the data, including the dates from Nazarovo site, so there is no indication of them being insufficiently bleached at deposition and, consequently, being overestimated.
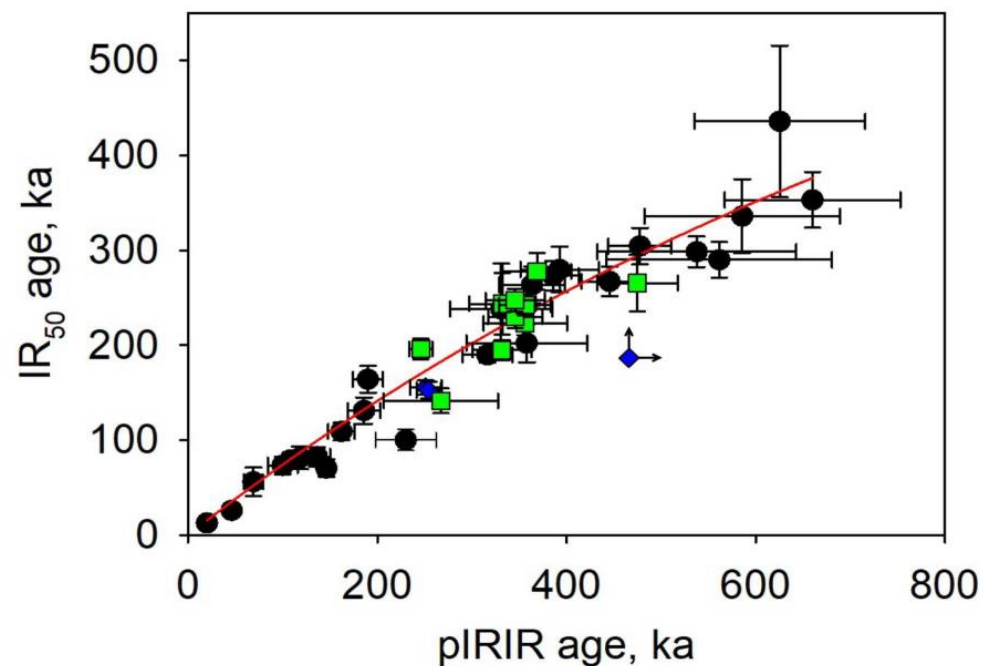
Figure 6. Feldspar pIRIR$_{290}$ and IR$_{50}$ ages comparison, adopted from [15], with added samples from Ilya Prorok site (blue diamonds) and Nazarovo site (green squares) highlighted. Black circles represent previous Volga dataset from [15]. Instead of the error bars, sample 208448 has two arrows indicating that its Feldspar ages are minimal.

3.1.4. Carpological Analysis

In the LCAs of samples from depths of 10.15 and 10.40 m from peat interlayers in the loam layer, unit 12 (Figure 5), the remains of eurythermal aquatic and wetland plants predominate (Figure 7). Several species of *Potamogeton* (*P. pusillus*, *P. gramineus*, *P.* cf. *perforatus*) are represented, and the seeds of *Myriophyllum verticillatum* are identified. Nutlets of sedge (*Carex* sp. div.) play a significant role, seeds of *Viola palustris* and fruits of *Urtica dioica* are found. Macroremains of tree species are represented by numerous nutlets and fruit scales of *Betula* sect. *Albae* and single nutlets of alder (*Alnus* sp.). No remains of thermophilic or cold-tolerant species were identified. Since the LCAs considered were found in the layers underlying the layer of dense gyttja, which, according to various researchers [12,23,25], corresponds to the warmest interval, these LCAs can be attributed to the initial phases of the interglacial.
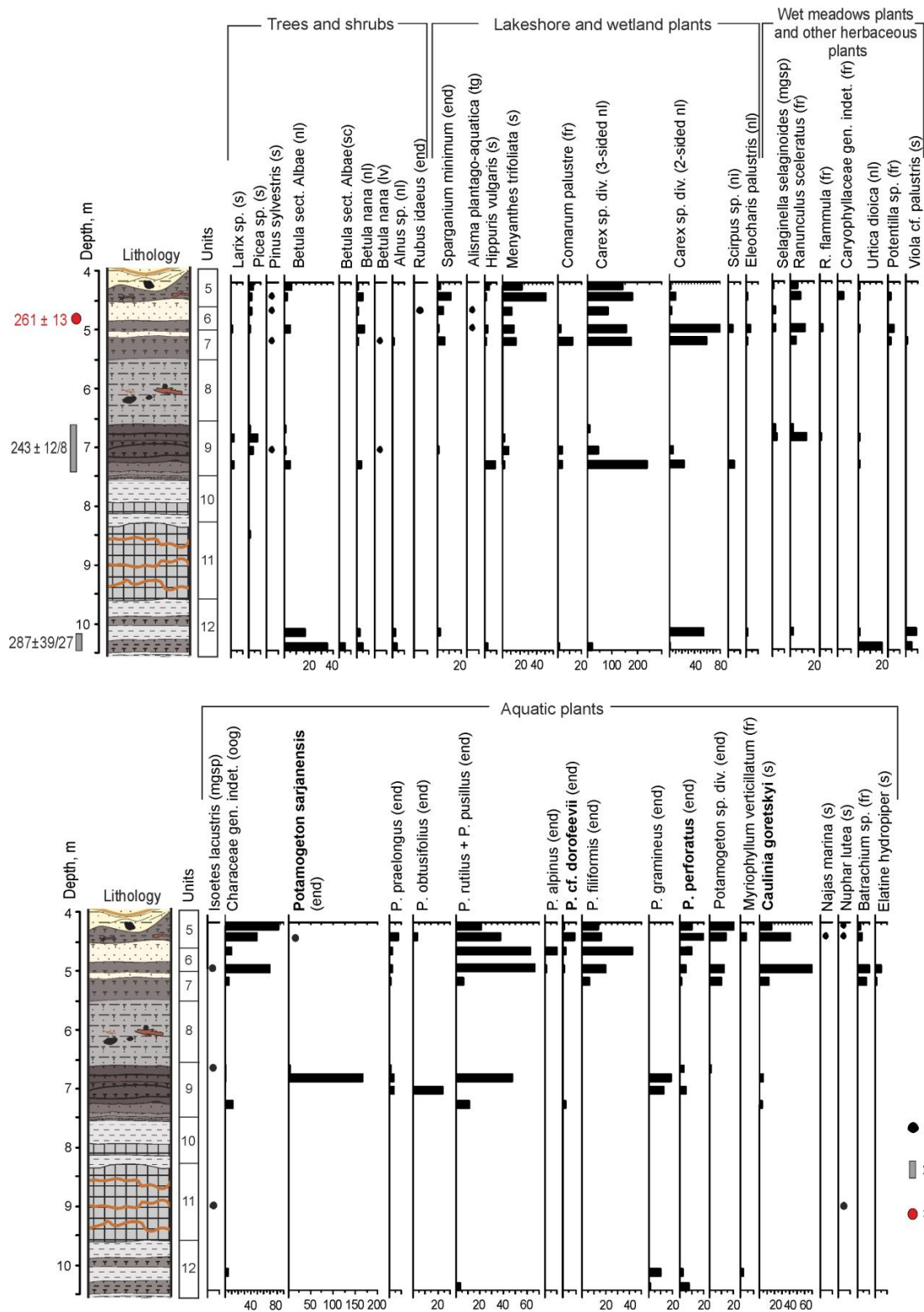
Figure 7. Carpological diagram of the IP-2015 section, Bolshaya Kosha (Ilya Prorok) exposure. See Figure 5 for lithology notations, Table 3 and Figure 5 for the numbers of lithostratigraphic units. Horizontal axes show number of specimens per sample. Legend: 1—scanty plant macroremains (<5 per sample), 2—^{230}Th/U dates, after [12], 3—IRSL date (this study), Abbreviations: s = seeds, fr = fruits, nl = nutlets, sc = fruit scales, oog = oogonia, mgsp = megaspores, tg = tegmens, end = endocarps, lv = leaves.

Two samples were collected from laminated mudstone at depths of 8.50 and 9.05 m (unit 10, Figure 5), where palynological data [12] suggested the presence of the main warming (potentially the Likhvin optimum). These samples, however, did not yield any plant macroremains.

The sample taken from a depth of 7.30 m (lower part of unit 9, Figure 5), consisting of leafy peat with a large amount of wood remains, exhibits a significant prevalence of palustrine plant macroremains. These are primarily represented by the nutlets of sedges (*Carex* sp. div.), as depicted in Figure 7. Some macrofossils of aquatic plants were identified, such as endocarps of pondweeds (*P. pusillus*) and fragments of seeds of *Caulinia* sp. The carpological remains of tree and shrub species are represented by scanty fruits of tree and dwarf birch (*Betula* sect. *Albae* and *B. nana*), as well as larch seeds (*Larix* sp.). The composition of this LCA indicates predominantly swampy local conditions and a relatively cool climate.

In the LCA of the sample taken from a depth of 7.05 m, there is a reduction in the quantity of sedge fruits, accompanied by an augmentation in the content and diversity of pondweed remains (*Potamogeton* cf. *perforatus*, *P. obtusifolius*, *P. gramineus*, *P. praelongus*). Rare remains of woody and shrub plants, such as fruits of birch (*B.* sect. *Albae*), spruce seed, and dwarf birch leaves were found (Figure 8). This LCA may indicate an increase in paleo-lake level in relatively cool climatic conditions.
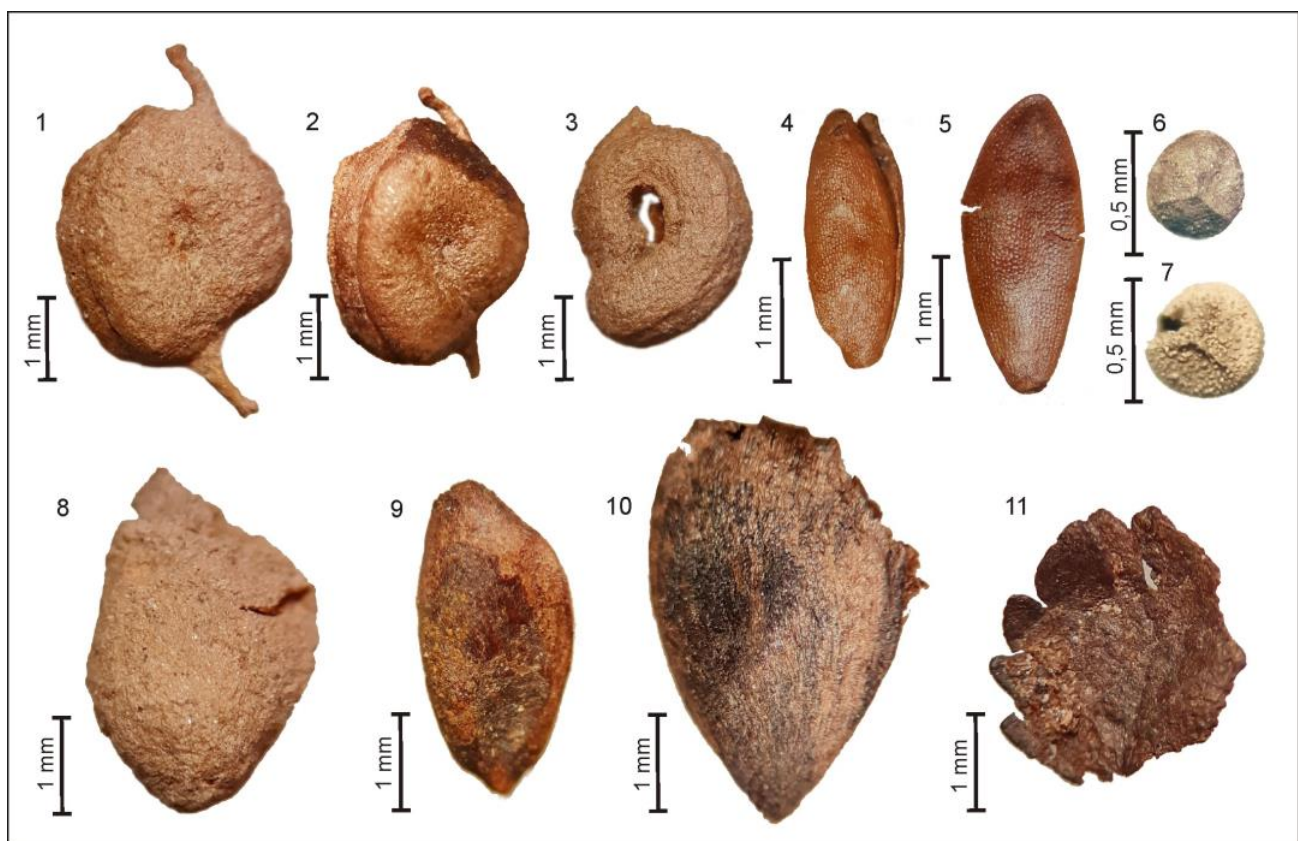
Figure 8. Plant macrofossils from the IP-2015 section, Bolshaya Kosha (Ilya Prorok) exposure. 1, 2—*Potamogeton sarjanensis* Wieliczk., endocarps; 3—*P.* cf. *perforatus* Wieliczk., endocarp; 4, 5—*Caulinia goretskyi* (Dorof.) Dorof., seeds; 6—*Isoetes lacustris* L., megaspore; 7—*Selaginella selaginoides* (L.) Beauv. ex Mart and Schrank, megaspore; 8—*Pinus sylvestris* L., seed; 9—*Picea* sp., seed; 10—*Larix* sp., seed; 11—*Betula nana* L., fragment of leaf.

In the LCA from the upper part of layer 9 (6.70–6.85 m), the content of pondweed endocarps continues to increase. Numerous endocarps of the extinct species *Potamogeton sarjanensis* (Figure 8) have been identified, as well as *P.* cf. *perforatus*, *P. pusillus*, etc. In addition, seeds of

another extinct species, *Caulinia goretskyi*, characteristic of the Likhvin Interglacial flora [32], were identified (Figure 7). Trees are represented by rare fruits of *B.* sect. *Albae* and *Larix* and *Picea* seeds (Figure 8). Findings of the hypoarcto-montane species *Selaginella selaginoides* megaspores (Figure 8) indicate fairly cool and humid climatic conditions. Macroremains of broad-leaved species, or of thermophilic aquatic and wetland plants, were not found in this layer.

The described LCAs are very similar to the carpological complexes identified by Velichkevich in 2003, from approximately the same depths [12].

In the LCAs from the upper part of the lacustrine–palustrine deposits (depth 4.20–5.20 m, layers 5–7, peaty loams, sands, and highly decomposed peat), the remains of wetland plants (*Carex* sp. div., *Menyanthes trifoliata*, etc.) predominate. However, the number and diversity of aquatic plant macrofossils is quite large, including Characeae gen. indet. (oogonia), endocarps of various pondweed (*P.* cf. *perforatus*, *P.* cf. *dorofeevii*, *P. praelongus*, *P. filiformis*, etc.), and *Batrachium* sp. (Figure 7). Seeds of an extinct species, *Caulinia goretskyi,* are found here in significant quantities. Tree species are still represented by sparse seeds of spruce, pine, and larch, as well as birch nutlets *(B.* sect. *Albae).* Almost all LCAs from this interval include nutlets of *Betula nana* and megaspores of *Selaginella selaginoides*. The considered LCAs reflect the conditions of a shallow, swampy lake that existed in relatively cold and humid climatic conditions. Carpological studies of this part of the section have not been previously carried out.

Additional samples from core 9, drilled in 2020, were also studied (Figure 4). Samples collected from peat layers at depths of 9.9–10.5 m (unit 9 in IP-2015, see Figure 5 and Table 3) contained rare macroremains of spruce (seeds and fragments of needles), as well as damaged seeds of *Caulinia* sp. In the sample taken from a depth of 8.1–8.4 m (unit 7 in IP-2015, see Figure 5 and Table 3), a few fruits of birch (*B.* sect. *Albae*), dwarf birch (*B. nana*), remains of wetland plants (*Carex* sp., *Menyanthes trifoliata*), and rare endocarps of aquatic plants (*Potamogeton* sp.) were registered.

3.2. Section Nazarovo

3.2.1. Geological Composition and Luminescence Age of Deposits

On the flat surface around the quarry, large boulders lie in groups, mostly with sandy matrix—the till of the Moscow glaciation (MIS 6) (Figure 9). Beneath it are beds of horizontally- and cross-bedded sands with interlayers of gravel, with a total thickness of 3.5 m. They are underlain by a 1 m thick layer composed of well-rounded boulders up to 30–40 cm in size, with a fill of fine sand. These two packs are interpreted as alluvial deposits that preceded the MIS 6 glaciation. IRSL dates from these layers mostly fall within the 330–370 ka interval, except for two outliers: 480 ± 40 ka and 270 ± 60 ka, with the latter date interval overlapping with the intervals of the majority of dates.

The core 19547, drilled at the bottom of the quarry, is located at an altitude of about 91 m asl. Under the basal boulder horizon of the upper alluvial unit, the core passed a typical alluvial sequence (Figure 9) of fine-grained overbank or oxbow-lake deposits at depths of 1.5–4.35 m, underlain by fine clayey horizontally layered sands with plant detritus (channel bar alluvium); below this, coarse sands with gravel (depth 5.5–7.0 m; active channel alluvium) and at the base, coarse material with sandy fill, which could not be penetrated by the core (basal alluvium). From this unit, similar IRSL ages of 330–360, with one outlier of 250 ± 10 ka, were obtained.

Thus, the section contains two alluvial units with an age of about 330–370 ka. According to the dates, this entire sequence falls into the transitional time from MIS 10 to MIS 9 (in the LR04 scale, the MIS 10—MIS 9 boundary is dated to 337 ka [7]), i.e., in the MIS 10 Late Glacial time.
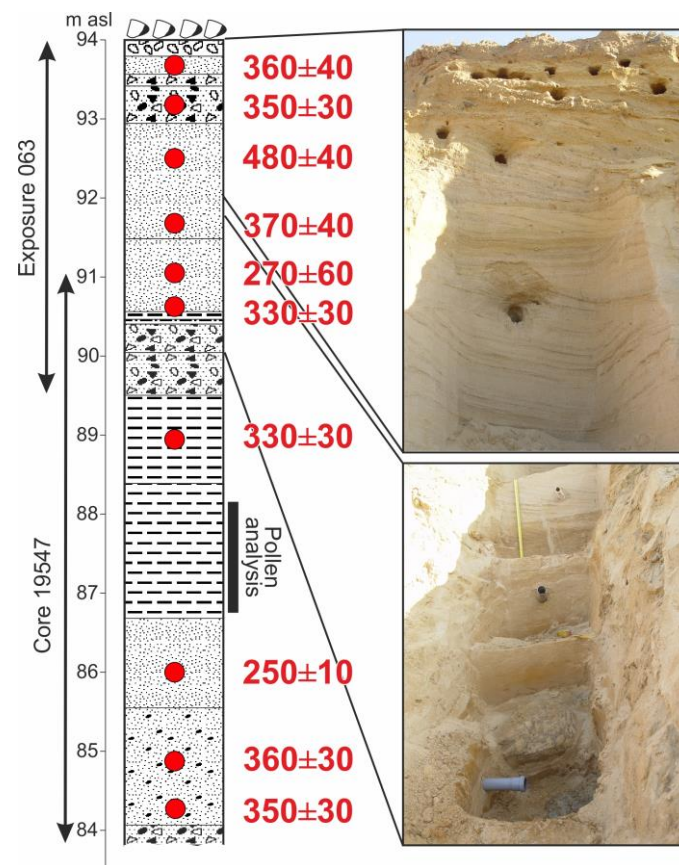
Figure 9. Section Nazarovo (core 19547). See Figure 3 for lithology notations. Red circles and numbers are IRSL dates, ka, according to [15]. Black strip indicates the interval of silty clay studied by pollen analysis.

3.2.2. Results of Spore/Pollen Study

The studied layer of heavy loam, with a thickness of about 1.5 m with lenses and layers of fine-grained sand in the lower part, lies in the depth range of 294–432 cm in core 19547, i.e., approximately at 87–88 m ASL (Figure 9). The general composition of the spectra is dominated by arboreal pollen (p.) (AP), which makes up 60–70% of the total amount of p. and spores (Figure 10). In this group, the most abundant is p. oa spruce (*Picea*), Scots pine (*Pinus sylvestris*), and birch (*Betula* sect. *Albae* and *B.* sect. *Fruticosae*). The relatively low preservation of pollen does not allow us to reliably distinguish the p. of birches of these two sections. In addition to the p. of conifers, approximately half of the studied samples contained their stomata, which could be identified to the taxonomic level of the genus.

Contents of non-arboreal p. (NAP) are almost constant throughout the entire section and do not exceed 20%. The main taxa in this group are *Artemisia*, Cyperaceae, Poaceae and, to a lesser extent, Chenopodiaceae. The content of spores (mainly *Sphagnum* and Polypodiaceae) is lowest in the lower part of the section (5–10%) and reaches a maximum in its middle part, where they account for about 15% of the total p. and spore sums. Based on changes in the composition of the spectra, three local pollen zones (LPZs) are clearly distinguished in the diagram.

In LPZ NZ-1, approximately corresponding to a layer of heavy loam with lenses of fine-grained sand, contents of birch, pine and spruce p. are approximately the same and do not exceed 15–25% of the spectra. In the sample from a depth of 416 cm, the *Larix* stomata were found. Since larch pollen have very low resistance to destruction, this find suggests the participation of larch in local vegetation, although no *Larix* p. was found in this zone. In LPZ NZ-1, the p. of shrubs (*B.* sect. *Nanae*, *Alnus* and/or *Alnaster* and *Salix*) occurs in small quantities. Rare pollen grains of relatively thermophile broad-leaved species (*Quercus*,

Tilia, *Carpinus*, *Corylus*) are found throughout the section without any visible pattern, which suggests that they were redeposited. Single pollen grains of *Fagus* and *Pterocarya* were also found in sandy loam at the base of the section. These tree species dropped out of the flora of this region after the Likhvin Interglacial and did not occur here in later interglacial epochs.
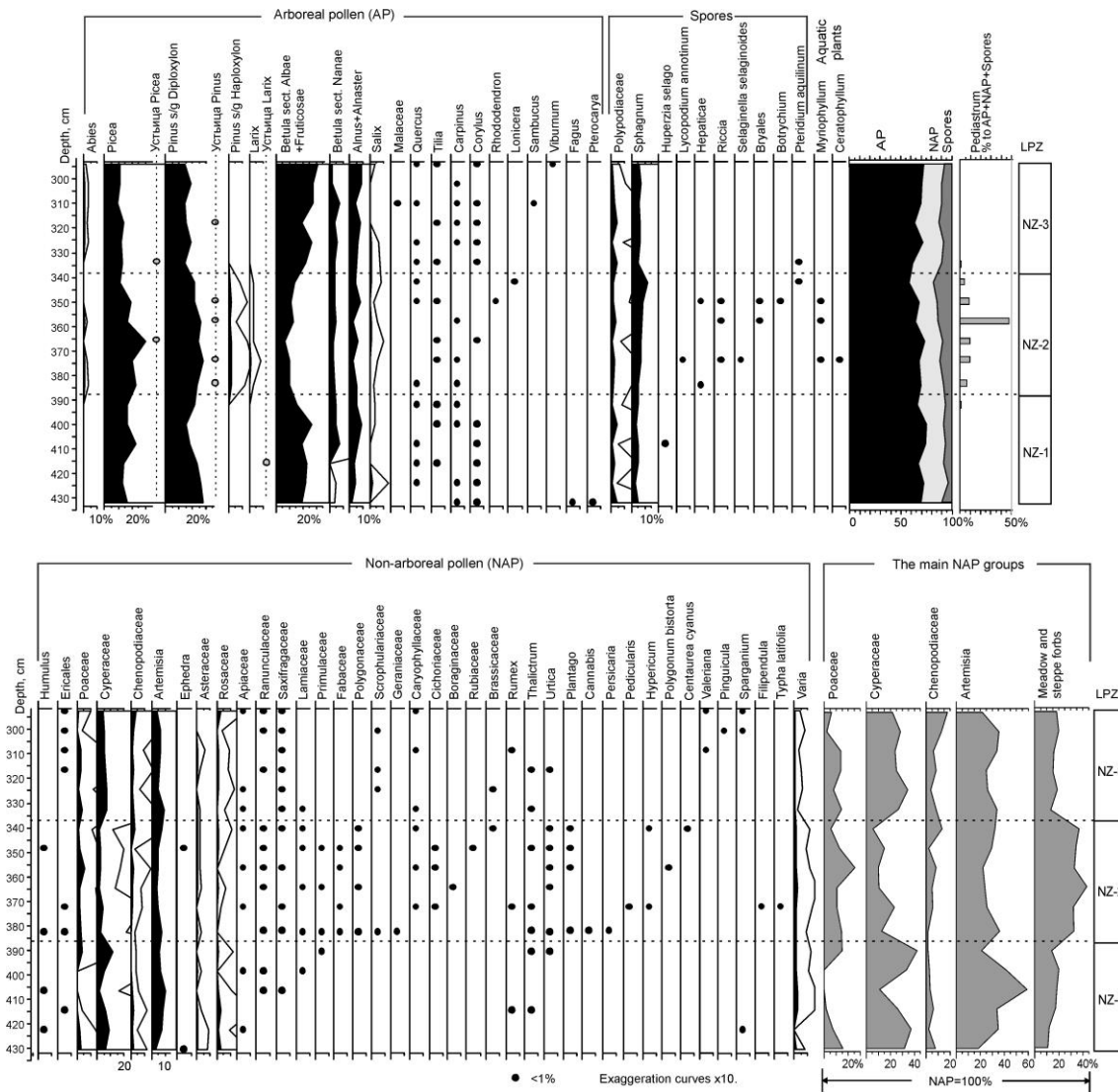
Figure 10. Pollen diagram of the Nazarovo (core 19547) section.

Composition of herbaceous plant pollen in LPZ NZ-1 is rather poor. Within the group, *Artemisia* predominates (up to 40% and about 60% of NAP in one sample) (Figure 10). However, such composition of the spectra in this zone, combined with the high pollen content of Cyperaceae (20–40% of NAP), shows that the abundance of *Artemisia* here can be explained not by the aridity of the climate, but by the intensive erosion and the presence of areas with disturbed or unformed soil cover near the section. The development of erosion processes is confirmed by the extraordinary diversity of redeposited ancient spores and pollen, as well as non-pollen palynomorphs (dinoflagellate cysts, foraminifers, etc.).

In LPZ NZ-2, the contents of *Picea* increased to 20–30% of the spectra. In the layer with the maximum of spruce pollen, *Picea* stomata were found, which confirms the increasing role of spruce in local vegetation. The composition of coniferous forests becomes richer; in LPZ NZ-2, pollen of *Pinus sibirica* and *Abies* is found. These tree species are typical of interstadial forest communities in the central regions of the East European Plain. The share

of *P. sylvestris* pollen also increases to 30% of the spectra, probably due to the increasing role of pine forests, possibly with an admixture of *Larix*, near the section, as pine stomata were found in most samples in this LPZ. Among the mesophilic shrubs, rare pollen grains of *Lonicera* and *Rhododendron* were found here.

Significant changes in the composition of herbaceous vegetation are reflected in a decrease in the proportion of *Artemisia* pollen to 20–30% of the NAP group, and in the increasing abundance and diversity of meadow herbs. Although this LPZ contains quite a lot of species, including inhabitants of places with disturbed soil (for example, *Centaurea cyanus*, *Cannabis*, *Plantago*, *Rumex*, *Ephedra*, etc.), in general, the composition of the spectra here reflects a decrease of the continentality of climate and increasing humidity, which is also emphasized by the increase in the number and diversity of spores. Among them there are species of clubmosses characteristic of dark coniferous forests (*Huperzia selago* and *Lycopodium annotinum*); *Pteridium aquilinum*, an inhabitant of light, mainly pine forests; *Sphagnum*, brown mosses and liverworts, and a hypoarctic species, *Selaginella selaginoides*.

The loam layer corresponding to LPZ NZ-2 probably accumulated in a small lake, as it contains pollen of aquatic and coastal plants (*Myriophyllum*, *Typha latifolia*), leaf spines of *Ceratophyllum*, and coenobia of the green algae *Pediastrum.* However, the low number of these palynomorphs and the small thickness of the layer that contains them (less than 0.5 m) show that this lake was short-lived, and the conditions in it were not favourable enough for the development of rich vegetation.

LPZ NZ-3 is very similar to LPZ NZ-1. Compared to LPZ NZ-2, the composition of coniferous forests becomes poorer (*P. sibirica* is absent) and their role in the composition of vegetation decreases. The share of pine forests is also decreasing, while birch formations expand. It is likely that larch is also falling out of local forest communities. Of the shrubs that inhabit the undergrowth of mixed and pine forests, the pollen of Viburnum and Sambucus is registered. Changes in the composition of NAP apparently reflect a local increase in soil moisture; Cyperaceae pollen reach 35% of the NAP group, while both the abundance and diversity of forbs are markedly reduced compared to LPZ NZ-2. Of the spores in this zone, only *Sphagnum* and Polypodiaceae are found, and the pollen of aquatic plants and green algae are completely absent here.

Thus, the palynological data obtained from the loam layer of the Nazarovo section reflect changes in the composition of vegetation from the northern to middle taiga forests, close to modern formations of Western Siberia that occurred during the relatively warm interstadial. The thickness of the studied layer of humified loams in the Nazarovo section is about 130 cm. Based on general considerations and comparisons with interstadial sections of the Late Pleistocene, including those dated by 14C, the duration of the warming represented in the pollen diagram for the Nazarovo section can be approximately estimated at 2 ka.

4. Discussion

4.1. Comparison of Middle Pleistocene Interstadial LCAs of the East European Plain

Carpological assemblages attributed to the transitional period between the Likhvin interglaciation and the subsequent glaciation are known in a number of sections of the East European Plain [25,51,52]. The LCA of the section near the village of Bulatovo, located near the Bolshaya Kosha section in the Selizharovsky district of the Tver region [51,53], is most similar in composition to the LCA of the IP-2015 section. According to palynological data, the Bulatovo section contains sediments of the climatic optimum of the Likhvin interglaciation, its post-optimum phase, subsequent cooling, and relative warming, which is considered to be an interstadial [51]. In the interglacial sediments of the Bulatovo section, in addition to extinct *C. goretskyi* and *C. interglacialis*, seeds of the extinct species *Aracites interglacialis*, exclusively characteristic of the flora of the Likhvin Interglacial and its analogues, were identified [25,32]. The remains of extinct species of *P. sarjanensis* and *C. goretskyi* [51,53] have been identified in the interstadial LCA of the Bulatovo section,

which were also found in the sediments of the Bolshaya Kosha section. It should be noted that in both sections, the seeds of *C. goretskyi* were found in both interglacial and "interstadial" sediments, whereas previously, seeds of *C. goretskyi* were known mainly in the LCA of the Likhvin Interglacial and its analogues, as well as in some older assemblages of the Lower Neopleistocene [25,32,54]. Endocarps of *P. sarjanensis* are known from sediments of the Belovezhyan Interglacial of the Lower Neopleistocene of Belarus, as well as from some sections of the Likhvin Interglacial and its analogues in Eastern Europe. These species do not occur in the flora of the Late Neopleistocene [32].

The presence of extinct aquatic species in the interstadial floras of the Bolshaya Kosha and Bulatovo sections does not contradict the conclusions about the relatively cold climatic conditions obtained from palynological data. Such species as *C. goretskyi* and *P. sarjanensis* could reappear in aquatic plant communities during short-term, relatively warm periods, against the background of the onset of the cold stage. Similar features were established earlier for seed floras of the Late Neopleistocene during the transition between the Mikulino Interglacial (MIS 5e) and the Early Valdai glaciations (MIS 4–5d) [25,55].

In general, the Middle Pleistocene interstadial LCAs of the Bolshaya Kosha and Bulatovo sections are characterized by a small amount of wood species remains, represented by seeds of spruce and pine, as well as fruits of birch *Betula* sect. *Albae*, the presence of macroremains of *Betula nana,* and megaspores of *Selaginella selaginoides*, as well as various macrofossils of aquatic and wetland plants.

Other sections of the Middle Neopleistocene are known in the territory of the East European Plain, where palaeobotanical data sufficiently characterize the Likhvin Interglacial and its analogues, followed first by climate cooling and then relative warming. The rank of these warmings is interpreted in different ways. For example, in the Tegliatsy (Tver Oblast, Kocha River) and Verkhovye and Ruba sections on the Western Dvina River, these warmings are regarded as interstadial [25,26]. In the key section of the Middle Pleistocene flora Prinemanskaya, similar warming is considered to be the second optimum of the Alexandrian (Belarusian analogue of the Likhvin) interglaciation, as macrofossils of some thermophilic species were identified in the corresponding sediments [52,56]. At the same time, E.M. Zelikson [57], based on palynological data, believes that this section represents an interglacial with one climatic optimum, and considers the later warming to be interstadial. The presence of thermophilic species in the "interstadial" flora of Prinemanskaya is explained by the milder climate in the territory of Belarus, compared to the Upper Volga basin. The number of distinguished interstadial warming periods varies from one to three [26]. Quantitative age estimates for the mentioned sections have not been yet obtained.

According to the reviewed paleobotanical data of different years, the section on the Bolshaya Kosha River quite fully represents the warming of the interglacial rank, which is associated with the Likhvin Interglacial [12,22,23,25,57]. In addition, palaeobotanical data ([12,23], present paper) reflect the subsequent cooling, against which a relative warming can be distinguished ("Koshinsky interstadial" by V.P. Grichuk [23]; see Table 2).

4.2. Interstadials of the Middle Pleistocene of the East European Plain According to Palynological Data

In the sequence of glacial–interglacial cycles, besides the main warm (actually interglacial) and cold (actually glacial) intervals, warm phases of shorter duration and amplitude are distinguished as interstadials, separated from interglacials and/or from each other by more or less pronounced cooling stages. The features of interstadial warmings that developed during the transition from interglacial to glaciation, and from glaciation to interglacial (that is, in the late glacial period of a particular glacial epoch), were discussed by E.M. Zelikson [57]. To determine the chronostratigraphic position of the Middle-Late Pleistocene interstadials, which are beyond the time span of radiocarbon dating, the most valuable are the palynologically studied sections, where the interstadial layers lie in a continuous sequence with interglacial deposits.

The features of the flora and vegetation of the interstadials "framing" the Likhvin Interglacial are discussed in detail in the article [58], based on palynological data from the Krukenichi section in the Dniester River basin. As in the Ilya Prorok section, the Kosha interstadial is clearly identifiable in the Krukenichi section. Unfortunately, in the Krukenichi section, there is a hiatus, as some part of the post-optimal phase of the Likhvin Interglacial is absent. The pollen characteristics of the Kosha interstadial are described in the article [57]. The same post-Likhvin interstadial is also distinguished in the pollen diagram from the Prinemanskaya section in Belarus.

In the Krukenichi section, a layer corresponding to a pre-Likhvin interstadial was also identified [58]. The late glacial part of the Oka Glaciation, transitional to the Likhvin Interglacial, is known from a few sections situated in the western parts of the East European Plain. Such an interstadial warming in the late part of the Oka Glaciation is distinguished on the pollen diagram from the Butenai section on the Šventoji River in Lithuania [58]. Spruce pollen contents during this interstadial reached 10% of AP. As the pollen record of the pre-Likhvin interstadial at Krukenichi shows similar characteristics to that at the Butenai section, V.P. Grichuk suggested to name this interstadial Sventoian. A similar warm interval has been recognised in the Prinemanskaya section in Belarus. The interstadial deposits at its base contain *Selaginella selaginoides*, *Betula nana*, *B.* sect. *Albae*, *Picea*, *Juniperus*, and other species [25]. Unfortunately, in one of the most detailed pollen diagrams from the Likhvin (Chekalin) key area, where a sediment thickness of more than 6 m underlying the Likhvin Interglacial layers was studied by M.P. Grichuk (the diagram was published in [59]), this interstadial is not expressed.

According to E.M. Zelikson [57], the climate of any period of short-term warming was determined by its position within the glacial–interglacial rhythm—interstadials preceding interglacials were more continental and arid than those following interglacials (they were more oceanic, though colder as compared with the interglacial). The changes in the composition of vegetation reflected these climate variations. Flora of the interstadials under consideration includes boreal and cryophilic elements, as well as xerophytes, primarily belonging to periglacial steppe group. Typical of the interstadials was complex vegetation; a combination of birch and pine (in the Middle Pleistocene, with *Larix*) forests and woodlands, communities of periglacial steppe formed by *Artemisia* of *Seriphidium* section, *Eurotia ceratoides*, *Kochia prostrata*, and others (with halophytes in the second half of glacial epochs), as well as communities of disturbed grounds. Spruce forests developed mainly in the interstadial optimums. Relative areas of plant communities depended on the interstadial position within the glacial–interglacial rhythm, forest communities being more widespread during interstadials that belonged to the early part of the glaciations.

The warming characterised by palynological data on the Nazarovo section can be attributed to a late glacial period, i.e., to the end of one of the glaciations. In addition to the changes of the pollen complexes in the section, the sediments contain very diverse redeposited Quaternary and Mesozoic microfossils (Filicales spores, dinoflagellate cysts, foraminifera, etc.), which indicate a high activity of erosion processes and open vegetation, a characteristic feature of a late glacial environment. In this case, the source of redeposition was probably till or glaciofluvial sediments containing already redeposited microfossils. The presence of pollen of various warm-temperate broad-leaved species among the redeposited microfossils and, in particular, the findings of pollen of *Fagus* and *Pterocaria*, the relict tree species that fell out of the flora of the East European Plain after the Likhvin Interglacial, allow us to conclude that the Nazarovo interstadial preceded this interglacial.

4.3. Geochronology of the Late Middle Pleistocene Warm Intervals in the East European Plain

The correlation of the Likhvin/Holstein interglaciation with the oxygen–isotope scale, and estimates of its duration, are still not in agreement. Most researchers correlate the Likhvin/Holstein interglaciation with MIS 11 [1,60–66], others with MIS 9 [5,67–69]. Quantitative age estimates obtained for section IP-2015 (Ilya Prorok, or Bolshaya Kosha exposure) by both ^{230}Th/U [12] and IRSL methods (as in this study) are approximately 250 to 290 ka

(central points of dates), fitting within MIS 8 [7]. However, these dates seem to underestimate the age of the sediments somewhat, even though there is no clear fault in the age data. Therefore, despite obtaining numerical ages, we still face some contradictions. A maximum possible ^{230}Th/U age estimate of 287 $\pm$ 39/27 ka was obtained from a peaty loam, which was assigned to the first half of the Likhvin Interglacial based on palaeobotanical data [12,22,23]. If we take the maximum boundary of the interval (287 + 39 = 326 ka), this date can be tuned to the MIS 9e interglaciation. The same interglacial is also indicated by ^{230}Th/U dating of Holstein sediments in Germany (Bossel section), according to which their age is 310–330 thousand years BP [67].

No dates were obtained directly from the slumped gyttja/argillite layer containing the most thermophilic Likhvin flora, but there are several dates from overlying layers, which, based on palynological [12] and carpological (this study) data, can be attributed to the relative warming within the post-Likhvin cold epoch (the Kosha interstadial). These are ^{230}Th/U dates 243 $\pm$ 12/8 ka, and IRSL dates 261 $\pm$ 13 and 249 $\pm$ 17 ka. According to palynological data, the section demonstrates quite regular climate cooling after the Likhvin Interglacial optimum in some parts of the section with a quite continuous sedimentological record [23], with only a small possible hiatus in other parts [12] (see Section 2.2). The cold event, ranked as glacial epoch, cannot be missed in this record. Therefore, the dates obtained by both methods appear to somewhat underestimate the age. This upper interstadial part of the section, in our opinion, belongs to the second half of MIS 9.

In the section near Chekalin (regional stratotype of the Likhvin Interglacial), the proper Likhvin layers containing interglacial flora were correlated with MIS 11 [25], and MIS 9 was compared with the buried soil horizon characterised by quite fragmentary spore/pollen data [65,70]. Sections of buried lacustrine deposits, which could be confidently compared with MIS 9e, are currently unknown in European Russia [26,65,70]. Therefore, we do not have reference floras for comparison of this interval. However, we obtained a close age for the interstadial sediments of the Nazarovo section, where IRSL dates are systematically older than those for the post-Likhvin interstadial sediments in the Bolshaya Kosha, indicating a pre-Likhvin age (Late Glacial MIS 10). The palynological data obtained in the Nazarovo section confirm the probability of the pre-Likhvin age of this interstadial.

The results of IRSL dating (Figure 9) suggest that the whole Nazarovo section below the MIS 6 till, including the layers characterised by pollen analysis, was formed in the interval 330–370 ka BP. These dates indicate that the palynologically characterised interstadial beds were very likely formed under Late Glacial conditions of MIS 10, before Termination IV, which is dated to 337 ka [3]. The dates from the post-optimal upper part of the IP-2015 section at Bolshaya Kosha refer to late MIS 9 (units 4–9, Figure 5). So, the studied interstadials bracket the MIS 9e interglacial, which probably refer to the deposits of the Likhvin climatic optimum in IP-2015 (units 11–12, Figure 5).

4.4. Correlation with the Middle Pleistocene Warm Epochs in Other European Sections

In Central Europe, the Holsteinian Interglacial is commonly correlated with MIS 11 (Table 1) [9,61,62,71]. Pollen data from the Shöningen paleolithic site reveal a two-phase warming (Interstadials Missaue I and II), following the initial post-Holsteinian cooling. These interstadials featured pine-birch forests with the participation of spruce [9]. Additionally, the Reinsdorf Interglacial, correlated with MIS 9, was identified at the same site [9,72,73]. Subsequently, stadial cooling occurred, marked by two interstadial-type climatic oscillations (Reinsdorf A and B), characterized primarily by the prevalence of pine forests [9]. The corresponding LCAs contain macroremains of *Pinus sylvestris*, *Frangula alnus*, *Rubus ideaus*, *Arctostaphylos uva-ursi*, and *Carex* sp. div. [74].

The Mazovian Interglacial in Poland, also correlated with MIS 11, is considered the stratigraphic analogue of the Holsteinian/Alexandrian/Likhvin Interglacial (Table 1) [8,61]. A continuous paleobotanical record, spanning the terminal phase of the Sanian-2 (Elster) glaciation, the entire Mazovian Interglacial, and the onset of the subsequent Liwiecian glaciation, was obtained from the Nowiny Žukowskie section [75]. According to pale-

obotanical data, two interstadials were distinguished at the beginning of the Liwiecian glaciation. Their LCAs contain numerous fruits of *Betula* sect. *Albae*, along with macroremains of *B. nana*, *B. humilis*, *Larix* sp., *Picea* sp., and *Pinus* sp. Aquatic and wetland plants are represented by remains of eurythermic and relatively thermophilic species [75]. The interstadial LCAs under consideration exhibit similarities to those from the Bolshaya Kosha and Bulatovo sections. However, LCAs of the initial post-Mazovian cooling and subsequent warming (interstadial 1) at the Nowiny Żukowskie site contain seeds of the extinct plant *Aracites interglacialis*, characteristic of the Likhvin/Alexandrian Interglacial of Eastern Europe [75]. It is possible that the climate in Central Europe was somewhat milder than that of Eastern Europe during this period.

To date, paleobotanical records, similar to those from the Reinsdorf sequence, "have barely been found in Germany or in the broader region" [73]. The series of ^{230}Th/U dates from buried peat in the Reinsdorf sequence spans from 280 to 343 Ka, corresponding to MIS 9 [72]. The biostratigraphic subdivision led to the conclusion that interglacial layers formed during substage MIS 9e [73]. However, a similar ^{230}Th/U age estimation (about 320 Ka) was obtained from buried fen peat in the Bossel section, the reference site for the Holsteinian Interglacial in Germany [67]. Although similar numerical age determinations were obtained from the Bolshaya Kosha sedimentary sequence using the IRSL method (present paper), we cannot confidently correlate this section with other Middle Pleistocene sections in Central Europe, due to regional differences in paleobotanical records.

5. Conclusions

The new data allow us to characterise the interstadial conditions preceding the MIS 9e interglacial epoch (Nazarovo section) and following it (upper part of the Bolshaya Kosha section). During the optimum of the Nazarovo interstadial, coniferous forests of complex composition with *Abies*, *Larix*, and *Pinus sibirica*, close to the modern middle taiga of Western Siberia, were developing. The cooling at the end of this interval led to the impoverishment of coniferous forests and the expansion of birch formations. According to the obtained series of IRSL dates, palynologically characterised fine-grained sediments (apparently floodplain lake sediments) accumulated for a short time (about two thousand years) within the 330–370 ka interval.

In the Bolshaya Kosha section, local carpological assemblages were revealed that probably belong to the initial phases of the Likhvin Interglacial. Layers corresponding to the optimum of the interglacial, according to palynological data [12,22,23], did not contain carpological remains. However, up the section, including the part that had not been subjected to carpological analysis before, rich LCAs typical of interstadial conditions of cold climatic epochs were found. At the same time, these LCAs contain the remains of some extinct species known from deposits of the Likhvin Interglacial and its analogues in Eastern and Western Europe. These features are representative of the carpological assemblages belonging to the transitional stage between the Likhvin interglaciation and the subsequent glaciation, as identified in a number of sections in the East European Plain [25].

The dates obtained by both the ^{230}Th/U method [12] and the IRSL method (this study) fall into MIS 8 and appear to us to somewhat underestimate the age of the sediments. If we increase the dates by 10–15%, they fall into different parts of MIS 9, from the interglacial optimum to the transition phase to the subsequent cold epoch. The lithological and palynological characteristics of the section show no evidence of a long hiatus between the sediments of the optimal interglacial phase and the post-optimal interstadials. On this basis, we assume that the optimum of the Likhvin interglaciation in the Bolshaya Kosha section (Ilya Prorok) belongs to MIS 9e (ca 330 ka), and the post-optimum warming ("Kosha Interstadial") belongs to MIS 9c or MIS 9a (280–310 ka) (MIS ages according to [3]).

References

1. Zastrozhnov, A.; Danukalova, G.; Shick, S.; Kolfschoten, T. State of stratigraphic knowledge of Quaternary deposits in European Russia: Unresolved issues and challenges for further research. *Quat. Int.* **2018**, *478*, 4–26. [CrossRef]
2. Lisiecki, L.E.; Raymo, M.A. Pliocene-Pleistocene stack of 57 globally distributed benthic D18O records. *Paleoceanography* **2005**, *20*, PA1003. [CrossRef]
3. Cohen, K.M.; Gibbard, P.L. Global chronostratigraphical correlation table for the last 2.7 million years, version 2019 QI-500. *Quat. Int.* **2019**, *500*, 20–31. [CrossRef]
4. Zhamoida, A.I.; Girshgorn, L.C.H.; Kovalevsky, O.P.; Oleynikov, A.N.; Prozorovskaya, E.L.; Margulis, L.S.; Khramov, A.N.; Shkatova, V.K. *Stratigraphic Code of Russia (Stratigraphicheskyi kodeks Rossii)*, 3rd ed.; VSEGEI Press: Sankt Petersburg, Russia, 2006; p. 95. (In Russian)
5. Velichko, A.A.; Morozova, T.D. Main features of soil formation during the Pleistocene on the East European Plain and their palaeo-geographical interpretation. In *Evolyutsiya Pochvi Pochvennogo Pokrova. Teoriya, Raznoobrazie Prirodnoi Evolyutsii i Antropogennykh Transformatsii Pochv*; Kudeyarov, V.N., Ivanov, I.V., Eds.; GEOS: Moscow, Russia, 2015; pp. 321–323. (In Russian)
6. Alekseev, A.S.; Shik, S.M. (Eds.) Resolution of regional interdepartmental stratigraphic commission (RISC) on the central and southern parts of the Russian platform Bureau on 16 March of 2010. *Bull. Regional Mezhved. Stratigr. Comm. po Centru i Yugu Russ. Platf.* **2012**, *5*, 10–18. (In Russian)
7. Lindner, L.; Gozik, P.; Jełowiczewa, J.; Marciniak, B.; Marks, L. Głowne problem klimatostratygrafii czwartorzedu Polski, Białorusi i Ukrainy. In *Geneza, Litologia i Stratygrafia Utworow Czwartorzedowych. Tom IV*; Wydawnictwo Naukowe Uniwersytetu im. Adama Mickiewicza: Poznan, Poland, 2004; pp. 243–258.
8. Marks, L.; Dzierżek, J.; Janiszewski, R.; Kaczorowski, J.; Lindner, L.; Majecka, A.; Makos, M.; Szymanek, M.; Tołoczko-Pasek, A.; Woronko, B. Quaternary stratigraphy and palaeogeography of Poland. *Acta Geol. Pol.* **2016**, *66*, 403–427. [CrossRef]
9. Urban, B. Interglacial pollen records from Schöningen, north Germany. In *The Climate of Past Interglacials*; Sirocko, F., Claussen, M., Sànchez Goni, M.F., Litt, T., Eds.; Elsevier: Amsterdam, The Netherlands, 2007; pp. 417–444. [CrossRef]
10. Ditmar, A.Y. Report on the geognostic study of Ostashkovsky, Rzhevsky, etc. counties. *Mat. Dlya Geol. Ross.* **1871**, *3*. (In Russian)
11. Khimenkov, V.G. Geological studies in the north-western and northern parts of 43 sheets of the 10-verst map of Russia. *Izv. Geol. Kom.* **1913**, *32*. (In Russian)
12. Maksimov, F.E.; Petrov, A.Y.; Grigoriev, V.A.; Konstantinov, E.A.; Kuznetsov, V.Y.; Arslanov, K.A.; Levchenko, S.B.; Karpukhina, N.V.; Starikova, A.A.; Baranova, N.G. ^{230}Th/U age and paleobotanic description of the organic-rich layer from the "Ilya Prorok" section on the Bolshaya Kosha River (Upper Volga basin). *Vestn. St. Petersburg Univ. Earth Sci.* **2022**, *67*, 243–265. [CrossRef]
13. Astakhov, V.; Shkatova, V.; Zastrozhnov, A.; Chuyko, M. Glaciomorphological Map of the Russian Federation. *Quat. Int.* **2016**, *420*, 4–14. [CrossRef]
14. Stolyarova, T.I. *Map of Quaternary Deposits. Sheet O-36-XXVIII, Scale 1:200,000 (Karta Chetvertichnyh Otlozhenij. List O-36-XXVIII, Masshtab 1:200,000)*; VSEGEI Press: Leningrad, Russia, 1961. (In Russian)
15. Utkina, A.O.; Panin, A.V.; Kurbanov, R.N.; Murray, A.S. Unexpectedly old luminescence ages as an indicator of the origin of the upper Volga River valley sediments. *Quat. Geochronol.* **2022**, *73*, 101381. [CrossRef]
16. Markov, K.K. Materials for the stratigraphy of Quaternary sediments of the Upper Volga basin. *Tr. Verkhnevolzhskoi Eksped.* **1940**, *1*, 4–38. (In Russian)
17. Moskvitin, A.I. Geological sketch of the Kalinin region. *Uch. zap. MGU* **1939**, *31*, 29–108. (In Russian)
18. Moskvitin, A.I. Odintsovo interglacial and the position of the Moscow glaciation among other glaciations in Europe. *Bull. Mosc. Soc. Nat. Geol. Ser.* **1946**, *21*, 79–98. (In Russian)
19. Moskvitin, A.I. *Wurmian Epoch (Neopleistocene) in the European Part of the USSR (Vyurmskaya Epoha (Neoplejstocen) v Evropejskoj Chasti SSSR)*; Izd-vo Akademii nauk SSSR: Moscow, Russia, 1950; pp. 53–56. (In Russian)
20. Stolyarova, T.I.; Gotfri, B.A.; Simonova, G.F.; Sooper, K.N.; Kalandadze, I.N.; Shipilov, I.I. *Report of the Selizhar Geological Survey Party (Ostashkovsky Detachment) on the Complex Geological Survey of the Mas-Headquarters 1:200,000 Sheet O-36-XXVIII, Produced*

in 1956–1957 (Otctet Selizharovskoi Geologo-Siomochnoi Partii (Ostashkovskii Otryad) o Kompleksnoi Geologicheskoi Siomke Masshtaba 1:200,000 Lista O-36-XXVIII, Proizvedionnoi v 1956–1957); GUCR: Moscow, Russia, 1958; p. 298. (In Russian)

21. Chebotaryova, N.S.; Nedoshivina, M.A.; Stolyarova, T.I. The Moscow-Valdai (Mikulin) interglacial deposits in the Upper Volga basin and their significance for paleogeography. *Byul. Kom. Po Izuch. Chetv. Per.* **1961**, *26*, 35–49. (In Russian)
22. Grichuk, V.P. Fossil floras as the basis for the Quaternary stratigraphy. In *Relief and Stratigraphy of the Quaternary Deposits in the North-Western Part of the Russian Plain (Rel'yef i Stratigrafiya Chetvertichnykh Otlozheniy Severo-Zapadnoy Chasti Russkoy Ravniny)*; Markov, K.K., Ed.; Izdatel'stvo AN SSSR: Moscow, Russia, 1961; pp. 25–71. (In Russian)
23. Grichuk, V.P. *History of Flora and Vegetation of the Russian Plain in the Pleistocene (Istoriya Flory i Rastitel'nosti Russkoj Ravniny v Plejstocene)*; Nauka: Moscow, Russia, 1989; p. 184. (In Russian)
24. Krasnov, I.I.; Kolesnikova, T.D. New data on interglacial deposits in the Upper Volga basin. *Byul. Kom. Po Izuch. Chetv. Per.* **1967**, *31*, 140–146. (In Russian)
25. Velichkevich, F.Y. *Pleistocene Flora of Glacial Regions of the East European Plain (Plejstocenovye Flory Lednikovyh Oblastej Vostochno-Evropejskoj Ravniny)*; Nauka i tekhnika: Minsk, Russia, 1982; p. 239. (In Russian)
26. Pisareva, V.V.; Sudakova, N.G.; Zyuganova, I.S.; Karpukhina, N.V.; Zakharov, A.L. Debatable problems of the Middle Pleistocene stratigraphy of the East European Plain's Central region. *Byul. Kom. Po Izuch. Chetv. Per.* **2019**, *77*, 49–85. (In Russian)
27. Konstantinov, E.A.; Mukhametshina, E.O.; Karpukhina, N.V. Conditions of occurrence and properties of buried organogenic sediments of the Bolshaya Kosha River basin (Tver region). *Est. i Tekhn. Nauk.* **2017**, *107*, 56–61. (In Russian)
28. Kozlov, V.B. Development of ancient lake basins on the territory of the Upper Volga. In *History of the Pleistocene Lakes of the East European Plain (Istoriya Plejstocenovyh ozer Vostochno-Evropejskoj Ravniny)*; Nauka: Sankt-Petersburg, Russia, 1998; pp. 335–340. (In Russian)
29. Pisareva, V.V. Reconstruction of paleolandscapes of the Likhvin interglacial and subsequent cooling in Eastern Europe. *Izv. RAN. Ser. Geogr.* **2012**, *3*, 54–70. (In Russian)
30. Grichuk, V.P.; Zaklinskaya, Y.D. *Analysis of Fossil Pollen and Spores and Its Application in Paleogeography (Analiz Iskopaemyh Pyl'cy i Spor i Ego Primenenie v Paleogeografii)*; OGIZ: Moscow, Russia, 1948; p. 223. (In Russian)
31. Nikitin, V.P. *Paleocarpological Method (Paleokarpologicheskij Metod)*; TGU: Tomsk, Russia, 1969; p. 82. (In Russian)
32. Velichkevich, F.Y.; Zastawniak, E. *Atlas of the Vascular Plant Macrofossils of Central and Eastern Europe, Part 1*; W. Szafer Institute of Botany: Kraków, Poland, 2006; p. 224.
33. Velichkevich, F.Y.; Zastawniak, E. *Atlas of the Vascular Plant Macrofossils of Central and Eastern Europe, Part 2*; W. Szafer Institute of Botany: Kraków, Poland, 2008; p. 380.
34. Grimm, E.C. *TGView, Version 2.0.2*; Illinois State Museum, Research and Collections Center: Springfield, IL, USA, 2004.
35. Dean, W.E. Determination of carbonate and organic matter in calcareous sediments and sedimentary rocks by loss on ignition; comparison with other methods. *J. Sediment. Res.* **1974**, *44*, 242–248.
36. Murray, A.; Arnold, L.J.; Buylaert, J.-P.; Guérin, G.; Qin, J.; Singhvi, A.K.; Smedley, R.; Thomsen, K. Optically stimulated luminescence dating using quartz. *Nat. Rev. Methods Primers* **2021**, *1*, 72. [CrossRef]
37. Hansen, V.; Murray, A.; Buylaert, J.-P.; Yeo, E.-Y.; Thomsen, K. A new irradiated quartz for beta source calibration. *Rad. Meas.* **2015**, *81*, 123–127. [CrossRef]
38. Hansen, V.; Murray, A.; Thomsen, K.; Jain, M.; Autzen, M.; Buylaert, J.-P. Towards the origins of overdispersion in beta source calibration. *Rad. Meas.* **2018**, *120*, 157–162. [CrossRef]
39. Thiel, C.; Buylaert, J.-P.; Murray, A.; Terhorst, B.; Hofer, I.; Tsukamoto, S.; Frechen, M. Luminescence dating of the Stratzing loess profile (Austria)—testing the potential of an elevated temperature post-IR IRSL protocol. *Quat. Int.* **2011**, *234*, 23–31. [CrossRef]
40. Buylaert, J.P.; Jain, M.; Murray, A.S.; Thomsen, K.J.; Thiel, C.; Sohbati, R. A robust feldspar luminescence dating method for Middle and Late Pleistocene sediments. *Boreas* **2012**, *41*, 435–451. [CrossRef]
41. Thomsen, K.J.; Murray, A.S.; Jai, M.; Bøtter-Jensen, L. Laboratory fading rates of various luminescence signals from feldspar-rich sediment extracts. *Rad. Meas.* **2008**, *43*, 1474–1486. [CrossRef]
42. Murray, A.S.; Marten, R.; Johnston, A.; Martin, P. Analysis for naturally occurring radionuclides at environmental concentrations by gamma spectrometry. *J. Radioanal. Nucl. Chem.* **1987**, *115*, 263–288. [CrossRef]
43. Murray, A.S.; Helsted, L.M.; Autzen, M.; Jain, M.; Buylaert, J.-P. Measurement of natural radioactivity: Calibration and performance of a high-resolution gamma spectrometry facility. *Rad. Meas.* **2018**, *120*, 215–220. [CrossRef]
44. Guerin, G.; Mercier, N.; Nathan, R.; Adamiec, G.; Lefrais, Y. On the use of the infinite matrix assumption and associated concepts: A critical review. *Rad. Meas.* **2012**, *47*, 778–785. [CrossRef]
45. Aitken, M.J. *Thermoluminescence Dating*; Academic Press: London, UK, 1985; p. 359.
46. Prescott, J.R.; Hutton, J.T. Cosmic ray contributions to dose rates for luminescence and ESR dating: Large depths and long-term time variations. *Rad. Meas.* **1994**, *23*, 497–500. [CrossRef]
47. Borisova, O.K.; Naryshkina, N.N.; Utkina, A.O.; Panin, A.V. On the diversity of interstadial environments of the Middle-Late Pleistocene in the Yaroslavl Volga region (according to palynological data). In *Proceedings of the XV All-Russian Palynological Conference Pending Problems of Modern Palynology*; Bolikhovskaya, N.S., Mamontov, D.A., Eds.; Lomonosov Moscow State University, GEOS: Moscow, Russia, 2022; pp. 91–96. (In Russian)
48. Murray, A.S.; Thomsen, K.J.; Masuda, N.; Buylaert, J.-P.; Jain, M. Identifying well-bleached quartz using the different bleaching rates of quartz and feldspar luminescence signals. *Rad. Meas.* **2012**, *47*, 688–695. [CrossRef]

49. Buylaert, J.-P.; Murray, A.S.; Gebhardt, A.C.; Sohbati, R.; Ohlendorf, C.; Thiel, C.; Wastegård, S.; Zolitschka, B. Luminescence dating of the PASADO core 5022-1D from Laguna Potrok Aike (Argentina) using IRSL signals from feldspar. *Quat. Sci. Rev.* **2013**, *71*, 70–80. [CrossRef]

50. Yi, S.; Buylaert, J.-P.; Murray, A.S.; Lu, H.; Thiel, C.; Zeng, L. A detailed post-IR IRSL dating study of the Niuyangzigou loess site in northeastern China. *Boreas* **2016**, *45*, 644–657. [CrossRef]

51. Kolesnikova, T.D.; Khomutova, V.I. Fossil Middle Pleistocene flora near the village of Bulatovo, Kalinin region. *Bot. Zhurn.* **1972**, *57*, 1422–1427. (In Russian)

52. Yakubovskaya, T.V. *Paleogeography of the Grodno Ponemanje's Likhvin Interglacial (Paleogeografiya Lihvinskogo Mezhlednikov'ya Grodnenskogo Poneman'ya)*; Nauka i Tekhnika: Minsk, Russia, 1976; p. 298. (In Russian)

53. Zyuganova, I.S. New data on the Middle Pleistocene flora of the Bulatovo section (Upper Volga basin). In *Problems of Modern Palynology: Materials of the XIII Russian Palynological Conference with International Participation (Problemy sovremennoj palinologii. Materialy HIII Rossijskoj Palinologicheskoj Konferencii s Mezhdunarodnym Uchastiem)*; IG Komi NC Uro RAN: Syktyvkar, Russia, 2011; Volume 2, pp. 108–111. (In Russian)

54. Field, M.; Velichkevich, F.; Andrieu-Ponel, V.; Woltz, P. Significance of Two New Pleistocene Plant Records from Western Europe. *Quat. Res.* **2000**, *54*, 253–263. [CrossRef]

55. Zyuganova, I.S. Early Valdai carpological assemblages from the Upper Volga Region. *Paleontol. J.* **2010**, *44*, 1368–1378. (In Russian) [CrossRef]

56. Elovicheva, Y.K. Continuous palynological record of paleogeographical events in the sediments of the paleolakes Kolodezhny (Belarus). In *Women Scientists of Belarus and Kazakhstan: Proceedings of International Scientific-Practical Conference (Zhenshhiny-uchenye Belarusi i Kazakhstana: Materialy Mezhdunarodnoj Nauchno-Prakticheskoj Konferentsii)*; Kazakova, I.V., Ed.; RIVSH: Minsk, Belarus, 2018; pp. 401–402. (In Russian)

57. Zelikson, E.M. Climate and environment changes of East Europe during interstadials and interglacials of the Middle and Late Pleistocene. In *Climate and Environment Changes of East Europe during Holocene and Late–Middle Pleistocene; Proceedings of the IGU Conference, Global Changes and Geography*; Institute of Geography RAS: Moscow, Russia, 1995; pp. 80–92.

58. Grichuk, V.P.; Gurtovaya, Y.Y. Interglacial lake-marsh deposits near the village of Krukenichi. In *Questions of Paleogeography of the Pleistocene Glacial and Periglacial Regions (Voprosy Paleogeografii Plejstocena Lednikovyh i Periglyacial'nyh Oblastej)*; Nauka: Moscow, Russia, 1981; pp. 59–91. (In Russian)

59. Ushko, K.A. Likhvinsky (Chekalinsky) section of interglacial lake sediments. In *Ice Age on the Territory of the European Part of the USSR and Siberia (Lednikovyj period na Territorii Evropejskoj Chasti SSSR i Sibiri)*; Izd-vo MGU: Moscow, Russia, 1959; pp. 148–226. (In Russian)

60. Lindner, L.; Bogucki, A.; Gozhik, P.; Marciniak, B.; Marks, L.; Lanczont, M.; Wojtanowicz, J. Correlation of main climatic glacial-interglacial and loess-palaeosol cycles in the Pleistocene of Poland and Ukraine. *Acta Geol. Pol.* **2002**, *52*, 459–469.

61. Nitychoruk, J.; Bińka, K.; Hoefs, J.; Ruppert, H.; Schneider, J. Climate reconstruction for the Holsteinian Interglacial in eastern Poland and its comparison with isotopic data from Marine Isotope Stage 11. *Quat. Sci. Rev.* **2005**, *24*, 631–644. [CrossRef]

62. Nitychoruk, J.; Bińka, K.; Ruppert, H.; Schneider, J. Holsteinian Interglacial = Marine Isotope Stage 11? *Quat. Sci. Rev.* **2006**, *25*, 2678–2681. [CrossRef]

63. Shik, S.M. Interglacial deposits of the center of European Russia (on the history of discovery and study). *Byul. Kom. Po Izuch. Chetv. Per.* **2005**, *66*, 98–106. (In Russian)

64. Coope, G.R.; Kenward, H.K. Evidence from coleopteran assemblages for a short but intense cold interlude during the latter part of the MIS11 Interglacial from Quinton, West Midlands, UK. *Quat. Sci. Rev.* **2007**, *26*, 3276–3285. [CrossRef]

65. Shik, S.M. A modern approach to the Neopleistocene stratigraphy and paleogeography of Central European Russia. *Stratigr. Geol. Correl.* **2014**, *22*, 219–230. [CrossRef]

66. Bolikhovskaya, N.S.; Molod'kov, A.N. Climate chronostratigraphic scheme of the Pleistocene of the East European Plain: Periodization, correlation and age of climatic events. In *Neogene and Flats of Russia: Stratigraphy, Events and Paleogeography (Neogen i Kvarter Rossii: Stratigrafiya, Sobytiya i Paleogeografiya)*; GEOS: Moscow, Russia, 2018; pp. 99–110. (In Russian)

67. Geyh, M.A.; Müller, H. Numerical ^{230}Th/U dating and a palynological review of the Holsteinian/Hoxnian Interglacial. *Quat. Sci. Rev.* **2005**, *24*, 1861–1872. [CrossRef]

68. Velichko, A.A.; Pisareva, V.V.; Faustova, M.A. Glaciations and interglacials of East European Plain in the Early and Middle Pleistocene. *Stratigr. Geol. Correl.* **2005**, *13*, 195–211.

69. Kühl, N.; Litt, T. Quantitative time series reconstructions of Holsteinian and Eemian temperatures using botanical data. In *The Climate of Past Interglacials*; Sirocko, F., Claussen, M., Sanchez Goñi, M.F., Litt, T., Eds.; Elsevier: Amsterdam, The Netherlands, 2007; pp. 239–254. [CrossRef]

70. Shik, S.M. On the paleobotanical characterization of the Post-Tikhvin interglacials of the Middle Pleistocene of the East European Plain. *Byul. Kom. Po Izuch. Chetv. Per.* **2014**, *73*, 77–86. (In Russian)

71. Koutsodendris, A.; Müller, U.C.; Pross, J.; Brauer, A.; Kotthoff, U.; Lotter, A.F. Vegetation dynamics and climate variability during the Holsteinian interglacial based on a pollen record from Dethlingen (northern Germany). *Quat. Sci. Rev.* **2010**, *29*, 3298–3307. [CrossRef]

72. Urban, B.; Sierralta, M.; Frechen, M. New evidence for vegetation development and timing of Upper Middle Pleistocene interglacials in Northern Germany and tentative correlations. *Quat. Int.* **2011**, *241*, 125–142. [CrossRef]

73. Urban, B.; Kasper, T.; Krahn, K.J.; Van Kolfschoten, T.; Rech, B.; Holzheu, M.; Tucci, M.; Schwalb, A. Landscape dynamics and chronological refinement of the Middle Pleistocene Reinsdorf Sequence of Schöningen, NW Germany. *Quat. Res.* **2023**, *114*, 148–177. [CrossRef]

74. Jechorek, H. Die fossile Flora des Reinsdorf-Interglazials. Paläokarpologische Untersuchungen an mittelpleistozänen Ablagerungen im Braunkohlentagebau Schöningen. *Praehistoria Thuring.* **2000**, *4*, 7–17.

75. Hrynowiecka, A.; Winter, H. Palaeoclimatic changes in the Holsteinian Interglacial (Middle Pleistocene) on the basis of indicator-species method—Palynological and macrofossils remains from Nowiny Żukowskie site (SE Poland). *Quat. Int.* **2016**, *409 Pt B*, 255–269. [CrossRef]